

POLITECNICO DI TORINO

Dipartimento di Ingegneria  
Corso di Laurea in Ingegneria Energetica e Nucleare

Tesi di Laurea Magistrale

# Remotization of a Solid Oxide Electrolytic Cell test bench and experimental characterization



**Relatore:**

Prof. Massimo Santarelli

**Correlatore:**

Prof. Domenico Ferrero

**Candidato:**

Angelo Danilo Nuzzolo

Matr. S270522

ANNO ACCADEMICO 2020-2021

## Summary

The European Commission presented in 2020 the European Green Deal, outlining the main policy initiatives for reaching net-zero global warming emissions by 2050. Hydrogen will be a key instrument for meeting the Green Deal objectives since it is considered by the international community as a carrier that can contribute to the decarbonization of the energy system. The aim of the sustainable plan is to have up to 14% of hydrogen from renewable sources in the final consumption mix, for this purpose, huge investments will be directed to electrolyzers system. In response of this new scenario, the analysis of a solid oxide electrolyzer arouses interest. Solid oxide fuel / electrolytic cells are completely solid state devices made of ceramic material conducting oxide ions. High temperatures (650-690 °C) are unavoidable to ensure good ionic conductivity; for this reason expensive components are required in the system with high temperature tolerance. The present experimental work can be divided into four main sections.

In the first section the working principle of fuel cells is presented with particular attention to the thermodynamic bases that characterize their operation. Furthermore, the polarization curve with the relative losses is shown.

In the second section the experimental activity held in the test bench is illustrated in details, analyzing the main components; in particular, the gas distribution system, the CEM (Controlled Evaporator Mixer), the auxiliaries, the cell housing and the control and acquisition system are examined.

In the third section the test bench control interface, based on Labview, is simulated by implementing a simple system consisting of flow meters / controllers, thermocouples, a data acquisition system and input / output modules. In the fourth section, it is analyzed a software to remotely control the test bench (EU project Teachy framework), the work in this case was based on system command / response tests in order to highlight any malfunctions in the operator interface.

Finally, the activity ends with the analysis carried out on the test bench, the experimental tests is performed by dividing the work in two main parts. The first part is determined by the calibration of those fundamental device for the correct functioning of the cell, such as mass flow controllers.

The second part is characterized by the assembly and the analysis of the cell. In particular the working session is based in testing the proper flow mixtures that feeds the Solid Oxide Electrolytic cell and the performance evaluation through the polarization curve analysis. Unfortunately, this last phase of experimentation is abruptly stopped due to the breaking of the cell. The corresponding result analysis highlights how the Solid Oxide Electrolytic cell strongly degrades during the operation.

# Table of contents

<b>Introduction</b>	<b>1</b>
<b>1 Fuel cell systems</b>	<b>4</b>
1.1 Thermodynamics . . . . .	4
1.2 Nernst Equation . . . . .	7
1.2.1 Fuel-cell Irreversibilities . . . . .	9
1.2.2 Activation Overpotential . . . . .	10
1.2.3 Internal current and fuel Crossover . . . . .	12
1.2.4 Ohmic Overpotential . . . . .	12
1.2.5 Mass transport losses . . . . .	13
1.2.6 Combining the Irreversibilities . . . . .	14
1.3 High temperature electrolysis . . . . .	14
1.3.1 Solid oxide electrolytic cell . . . . .	15
1.4 State of art . . . . .	17
1.4.1 Electrolyte . . . . .	19
1.4.2 Anode . . . . .	20
1.4.3 Cathode . . . . .	21
1.4.4 Interconnect material . . . . .	21
1.4.5 Sealing materials . . . . .	23
<b>2 Test bench experimental setup</b>	<b>24</b>
2.1 Gas distribution system . . . . .	25
2.1.1 Mass flow controller . . . . .	25
2.1.1.1 Working principle . . . . .	27
2.1.2 Risks Analysis for an explosive environment . . . . .	27
2.2 CEM . . . . .	28
2.2.1 CEM working principle . . . . .	29
2.3 Oven and test cell . . . . .	31
2.3.1 Eurotherm . . . . .	31
2.3.2 Test Housing . . . . .	33
2.4 Electric auxiliaries . . . . .	34

2.5	Acquisition and Control system . . . . .	35
2.5.1	Local software and hardware . . . . .	35
2.5.1.1	PID control . . . . .	36
2.5.2	Development of ‘remote lab’ concept . . . . .	36
<b>3</b>	<b>Labview Simulation and Teachy software</b>	<b>40</b>
3.1	LabVIEW (National instruments) Hardware . . . . .	40
3.2	LabVIEW (National instruments) Software . . . . .	43
3.2.1	Front Panel . . . . .	43
3.2.2	Block diagram . . . . .	44
3.2.3	Icon and connector pane . . . . .	45
3.3	Case study . . . . .	46
3.3.1	Acquisition - DAQ Assistant . . . . .	46
3.3.2	Data analysis . . . . .	47
3.3.3	Control output . . . . .	48
3.3.4	While loop . . . . .	50
3.3.5	Further implementation . . . . .	50
<b>4</b>	<b>Teachy Software</b>	<b>52</b>
4.1	Dashboard . . . . .	54
4.1.1	Menu account Root . . . . .	54
4.1.2	Menu account Administrator . . . . .	54
4.1.3	Menu account User . . . . .	56
4.2	Teachy items Description . . . . .	56
4.2.1	Home . . . . .	57
4.2.2	Account Management . . . . .	57
4.2.2.1	Admins List / Users List . . . . .	57
4.2.3	Account Creation . . . . .	58
4.2.3.1	Creation Admin/user . . . . .	58
4.2.4	Variables Management . . . . .	59
4.2.4.1	Variable list . . . . .	59
4.2.4.2	Create variable . . . . .	59
4.2.5	Groups Management . . . . .	59
4.2.5.1	Groups list . . . . .	60
4.2.5.2	Create group . . . . .	61
4.2.5.3	Assign User . . . . .	61
4.2.6	Experiment profile . . . . .	62
4.2.6.1	Experiment list . . . . .	62
4.2.6.2	Create Experiment profile . . . . .	63
4.2.7	Script . . . . .	64
4.2.8	Experiment section . . . . .	64

4.2.8.1	Experiment section Administrator . . . . .	64
4.2.8.2	Experiment section User . . . . .	66
4.2.9	Logs configuration . . . . .	66
4.2.10	Command . . . . .	68
4.2.11	Log . . . . .	68
<b>5</b>	<b>SOEC test</b>	<b>70</b>
5.1	Mass flow controllers Calibration . . . . .	70
5.2	Setting up procedure . . . . .	76
5.3	Start-up procedure . . . . .	81
5.3.1	Cell conditioning . . . . .	81
5.3.2	Cell reduction and activation . . . . .	81
5.4	Cell testing . . . . .	83
5.4.1	Flow setting . . . . .	84
5.4.2	Polarization . . . . .	85
5.5	Shut-down procedure . . . . .	86
	<b>Conclusions</b>	<b>87</b>
	<b>Bibliography</b>	<b>89</b>

# List of figures

1	Phosphoric acid fuel cell for stationary power-plant applications [2]. . . . .	2
2	Global annual demand for hydrogen (pure or as part of mixed gases) by application [4]. . . . .	3
1.1	The reversible fuel cell, its energy balance and its system boundary . . . . .	5
1.2	SOFC working principle [6] . . . . .	6
1.3	Polarization curve [2] . . . . .	9
1.4	Steam electrolysis ideal energy requirement . . . . .	15
1.5	Schematic of SOEC Hydrogen production [13]. . . . .	16
1.6	Anode and cathode reaction for SOFC, using both hydrogen fuel [2] . . . . .	18
1.7	Anode and cathode reaction for SOFC, using carbon monoxide fuel [2] . . . . .	18
1.8	Anode supported cell state of art . . . . .	19
1.9	Structure of yttria-stabilized zirconia [2] . . . . .	20
1.10	Cubic perovskite structure representation [2]. . . . .	22
1.11	Cell structure [15]. . . . .	22
1.12	Glass Sealing material [17] . . . . .	23
2.1	Schematic block diagram indicating the main subsystems. . . . .	24
2.2	Gas distribution connection . . . . .	26
2.3	Swagelok fitting . . . . .	26
2.4	The EL-FLOW Select series Mass Flow Meters and Controllers for gas applications [18]. . . . .	27
2.5	Mass flow controller working principle [18]. . . . .	28
2.6	Danger cones . . . . .	29
2.7	CEM connection. . . . .	30
2.8	CEM connection with liquid flow meter. . . . .	30
2.9	CEM working principle [19]. . . . .	31
2.10	Cell placed in the oven . . . . .	32
2.11	Eurotherm [20] . . . . .	32
2.12	Automatic Control loop [21] . . . . .	33
2.13	Pipes connected with twisted cables. . . . .	34

2.14	Representation of the metal grid, insulating frame and platinum wire for voltage measurement. . . . .	34
2.15	Manual control panel. . . . .	37
2.16	SOEC and SOFC electronic circuits . . . . .	38
2.17	Manual control panel: PID . . . . .	39
2.18	CompactRio . . . . .	39
2.19	Remote control system scheme . . . . .	39
3.1	Labview cyber signals . . . . .	41
3.2	Mass flow controller electrical connection . . . . .	42
3.3	Mass flow meter electrical connection . . . . .	42
3.4	Case study: Front Panel. . . . .	44
3.5	Case study: Block diagram. . . . .	46
3.6	DAQ Assistant block . . . . .	47
3.7	Thermocouples B and K setup . . . . .	47
3.8	Current input setup . . . . .	47
3.9	Schematic block diagram with subsystems . . . . .	48
3.10	Front panel user interface . . . . .	49
3.11	Current Output Setup . . . . .	49
3.12	Mass flow rate selection and consequentially block diagram. . . . .	49
3.13	Experiment time duration and consequentially block diagram. . . . .	50
3.14	Cumulated volume block diagram. . . . .	50
3.15	Alarm indicators related to temperature (right side) and mass flow rate (left side). . . . .	51
3.16	Compact DAQ during the operation. . . . .	51
4.1	Teachy Architecture. . . . .	53
4.2	Teachy Login. . . . .	53
4.3	Menu account Root. . . . .	54
4.4	Menu account Administrator. . . . .	56
4.5	Menu account User. . . . .	57
4.6	Admin list (right side) and User list (left side). . . . .	58
4.7	Admin Account Creation. . . . .	58
4.8	Variable list (right side) and Variable list in maintenance mode (left side). . . . .	59
4.9	New variable creation . . . . .	60
4.10	New variable creation . . . . .	60
4.11	Group list. . . . .	61
4.12	Group creation. . . . .	62
4.13	Assign User list. . . . .	62
4.14	Assign User type. . . . .	63

4.15	Experiment profile List. . . . .	63
4.16	Create Experiment profile. . . . .	64
4.17	Script section. . . . .	65
4.18	Condition to run the script (right side) and condition to stop the script (left side). . . . .	65
4.19	Experiment section Administrator. . . . .	66
4.20	Experiment section User. . . . .	67
4.21	Logs configuration. . . . .	67
4.22	Command section. . . . .	68
4.23	Log section. . . . .	69
4.24	Log chart. . . . .	69
5.1	Definer 220 [24] . . . . .	71
5.2	Cathode and Anode Manifolds representation. . . . .	76
5.3	Superglue application and seal placing on the manifold. . . . .	77
5.4	Mesh placing. . . . .	77
5.5	Cell alignment. . . . .	78
5.6	Mesh and seal placing onto cathode active area. . . . .	78
5.7	Collocation of the flexible insulation. . . . .	79
5.8	Manifold alignment. . . . .	79
5.9	Insulating ceramic cloth tubes deployment. . . . .	80
5.10	Housing of the test cell. . . . .	80
5.11	Start-up script. . . . .	82
5.12	Setup variables windows. . . . .	82
5.13	Eurotherm windows . . . . .	83
5.14	Cell reduction and activation script. . . . .	84
5.15	SOEC flow setting. . . . .	85
5.16	SOEC shut-down. . . . .	86

# List of tables

5.1	MFC 1 calibration. . . . .	71
5.2	MFC 2 calibration. . . . .	72
5.3	MFC 3 calibration. . . . .	72
5.4	MFC 4 calibration. . . . .	73
5.5	MFC 6 calibration. . . . .	73
5.6	MFC 7 calibration. . . . .	74
5.7	MFC 5 calibration. . . . .	74
5.8	MFC 10 calibration. . . . .	75
5.9	MFC 8 calibration. . . . .	75
5.10	CEM flow mixture and temperature computation. . . . .	85

# Introduction

Heavy dependence on finite fossil fuels as the major source of energy has caused serious energy crisis in the world. On the other hand, the combustion of fossil fuels for power generation poses unresolved impact on the climate. In order to mitigate these two problems, it is increasingly urgent to explore and utilize clean and renewable energy sources. Solar energy and wind power are the most plentiful renewable resources and thus are most promising for replacing existing fossil fuel-based energy sources. Solar and wind power are site-specific, intermittent, and thus are not reliable for instantaneous supply of energy. Using batteries to store any energy surplus for later consumption can resolve the time mismatch between energy supply and demand.

However, the deficiencies of battery storage are low storage capacity, short lifetime, and a big amount of wastes generated.

In order to better harness the variable amount of renewable energy, hydrogen has been identified as a potential alternative fuel as well as an energy carrier for the future energy supply.

Hydrogen is clean and, in practice, it can be produced from water, which is abundant. When it is converted into useful electricity via a fuel cell, the by-product is harmless water. But today, hydrogen is mainly produced from fossil fuels, i.e. natural gas steam reforming. However, the reforming of fossil fuels is neither renewable nor clean (Steam Methane Reforming (SMR) is the most commonly employed process globally for hydrogen production).

Hydrogen can be produced in a more environmentally friendly manner by water electrolysis, thermochemical water splitting, and photocatalytic water splitting. Water electrolytic hydrogen is so far the most practical and promising technology for large-scale renewable hydrogen production [1]. For all types of fuel cell, a significant disadvantage or barrier to commercialization is the capital cost.

There are, however, various beneficial points that allow the fuel cells to be attractive for different applications:

- *Efficiency.* Fuel cells are generally more efficient than traditional combustion engines.

A further benefit is that small fuel-cell systems can be just as efficient as

---

large ones. This capability opens up a market opportunity for small-scale cogeneration (CHP) that cannot be satisfied with turbine- or engine-based systems.

- *Low emissions.* When hydrogen is the fuel, pure water is the by-product of the main reaction of the fuel cell. Consequently, the power source is essentially ‘zero emission’. This is a particularly attractive for vehicle applications. Nevertheless, it should be noted that, considering the total life cycle of hydrogen production, emissions of carbon dioxide are nearly always present.
- *Simplicity.* The essentials of a fuel cell involve few, if any, moving parts. This can lead to highly reliable and long-lasting systems.
- *Silence.* Fuel cells are very quiet, this is due to the fact that they don’t have moving parts. Quietness is very important in both portable-power applications and for local power generation via CHP schemes [2].

In summary, the advantages of fuel cells impact particularly strongly on CHP systems (fig.1) (both large and small scales) and on mobile power systems — especially for vehicles and electronic equipment such as portable computers, mobile telephones and military communications equipment [2].,



Figure 1: Phosphoric acid fuel cell for stationary power-plant applications [2].

The Hydrogen is considered as an important feedstock for several processes including ammonia production and crude oil refining, transportation, and power-to-gas applications. The first two industries mentioned currently consume approximately

80% of the hydrogen produced globally. Approximately 65 million tonnes of H<sub>2</sub> is produced annually in the world, and the global rate of hydrogen consumption has increased by approximately 3-4% annually since 2003. [3].

In 2018 the global hydrogen demand has risen above 70 MMT for pure hydrogen and above 40 MMT for hydrogen in mixed gases (fig.2).

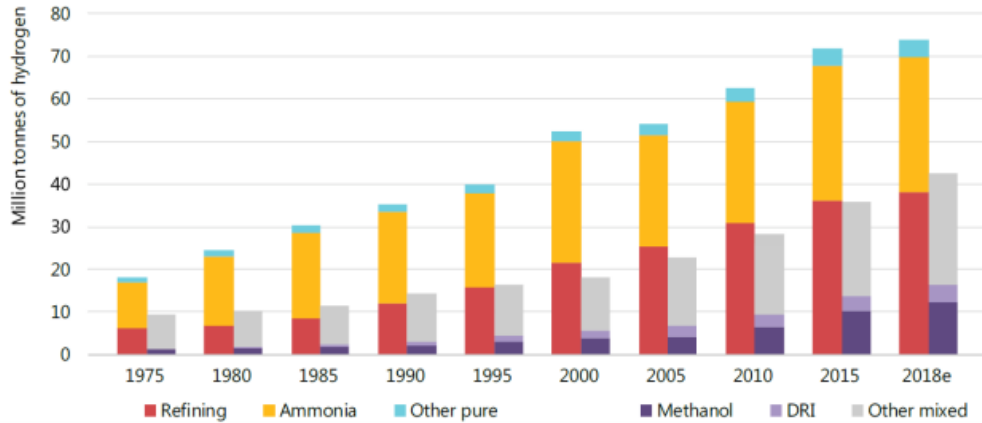


Figure 2: Global annual demand for hydrogen (pure or as part of mixed gases) by application [4].

In the present experimental work a test bench was developed for testing a high temperature cell and a web interface is created to remotely control the system. The paper is divided into five chapters:

1. In the first chapter a Thermodynamic analysis is carried out pointing out the performances and losses of a solid oxide fuel cell, with particular attention of irreversibility during the operation. The chapter concludes by examining solid oxide cell state of art.
2. In the second chapter are analyzed the main components of the test bench; including the gas distribution system, the Controlled Evaporator Mixer, the electronic system, the cell housing, and the control and acquisition system.
3. In the third chapter is created a simple system to simulate the test bench control interface with Labview software.
4. The the fourth chapter is characterized by the analysis of a software to remotely control the test bench (EU project Teachy framework).
5. The last chapter resumes those procedures for assembly and analysis of a SOEC and the associated script generated in *Teachy script editor* platform to remotely control the test bench.

# Chapter 1

## Fuel cell systems

### 1.1 Thermodynamics

The use of the first and the second laws of thermodynamics allows a simple description of a reversible fuel cell. In a reversible fuel cell the fuel and the air enters and leaves system without mixing each other

The specific enthalpy is delivered by the non-mixed reactants  $\sum_i(\dot{n}_i h_i)$  to the fuel cell and extracted by the non-mixed products (where  $\dot{n}_i$  is the molar flow). Furthermore the heat  $\dot{Q}_{rv}$ , is extracted reversibly from the fuel cell and transported to the environment [5]. The reversible work  $\dot{W}_{rv}$  instead, is delivered by the fuel cell (as shown in fig 1.1). This simplified condition occurs, if the fuel cell and the environment have the same thermodynamic state. Applying the steady flow energy equation with the assumption of negligible change of kinetic energy and potential energy, the first thermodynamic law is obtained.

$$\dot{Q}_{rv} - \dot{W}_{rv} + \sum_i(\dot{n}_i h_i)_R - \sum_i(\dot{n}_i h_i)_P = 0 \quad (1.1)$$

The entropy balance can be written as:

$$\frac{\dot{Q}_{rv}}{T} - \sum_i(\dot{n}_i s_i)_R - \sum_i(\dot{n}_i s_i)_P = 0 \quad (1.2)$$

Combining the two equations and since there is no mechanical work involved,  $\dot{W}_{rv}$  will be naturally the electrical work done by the fuel cell, that is:

$$W_{el} = -(\Delta H - T_{cell}\Delta S) = -\Delta G \quad (1.3)$$

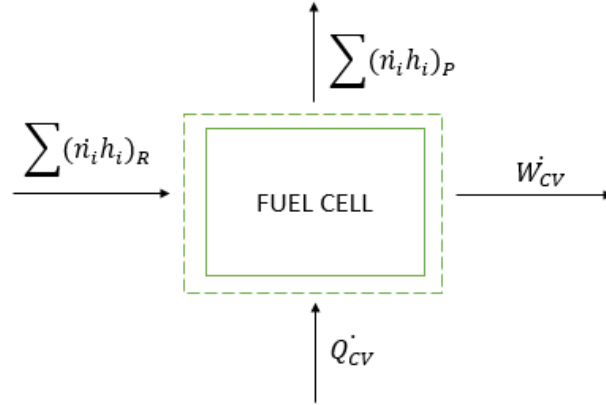
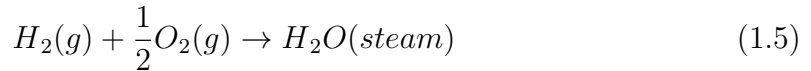


Figure 1.1: The reversible fuel cell, its energy balance and its system boundary

This expression is known as the ‘Gibbs equation’, where  $\Delta H$  is the change in enthalpy,  $\Delta S$  is the change in entropy between reactants and products, and  $T$  is the absolute temperature, finally  $\Delta G$  can be considered as the maximum reversible work that may be performed by a thermodynamic system at a constant temperature and pressure. This equation leads to definition of fuel cell reversible efficiency  $\eta_{cv}$  as the ratio between the Gibbs free energy of reaction and the change in enthalpy:

$$\eta_{cv} = \frac{\Delta G}{\Delta H} = \frac{\Delta H - T_{cell} \Delta S}{\Delta H} \quad (1.4)$$

The black box represented in figure 1.1 represent an high temperature electrochemical cell. The solid oxide fuel cell (SOFC) under consideration consists of two electrodes sandwiched around a hard ceramic electrolyte such as the remarkable ceramic material called zirconia. The fuel cell working principle is based on the following overall reaction:



The overall reaction does not change even if the fuel cell types is modified. The difference between various fuel cell technology is detected by highlighting the half reaction in the anode and cathode side. In the case of SOFC, the presence of zirconia in the electrolyte allows the conduction of oxygen ions ( $O_2^-$ ), for this reason the half chemical reaction in the anode and cathode will be respectively:





Hydrogen fuel is fed into the anode and oxygen, from the air, into the cathode. Oxygen in the air combines with free electrons to form oxide ions at the cathode. Oxide ions with free electrons travel from the cathode to the anode through the electrolyte. At the anode, oxide ions react with hydrogen forming water (steam). The oxidation reactions release free electrons which travel to cathode through the external electrical circuit, producing electricity. The overall reaction is displayed in the figure 1.2.

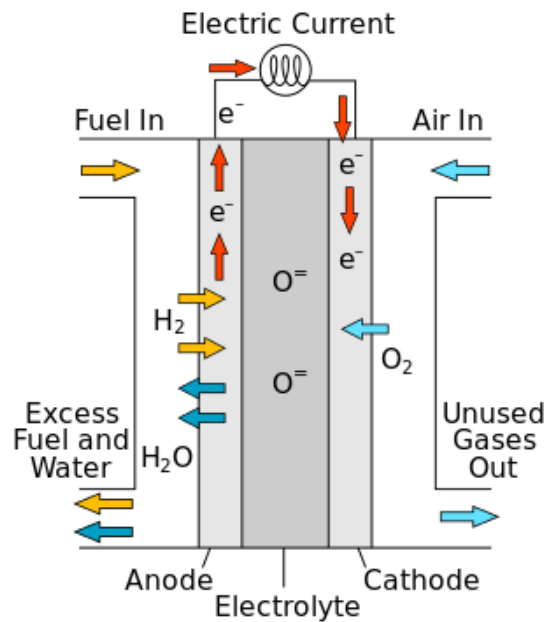


Figure 1.2: SOFC working principle [6]

As shown the equation (1.6), for each hydrogen molecule used two electrons travel round the external circuit for each water molecule produced. Thus, for each mole of hydrogen consumed,  $2N_A$  electrons pass round the external circuit. Given that each electron carries a unit negative charge ( $e^-$ ) the corresponding charge, in coulombs (C), that flows is:

$$- 2N_A e^- = -2F \quad (1.8)$$

where  $F$  is the Faraday constant or the charge on 1 mol of electrons. If 'V' is the

fuel cell voltage, then the electrical work, in joules (J), paid in moving this charge round the circuit is:

$$\text{Electrical work} = \text{charge} * \text{voltage} = -2F \quad (1.9)$$

Considering the system as thermodynamically reversible (with no energy losses), then the electrical work done will be equal to the Gibbs free energy released by the fuel-cell reaction  $\Delta\bar{g}_f$ . Thus:

$$\Delta\bar{g}_f = -2FV_r \quad (1.10)$$

This fundamental equation gives the ‘reversible voltage’,  $V_r$ , or ‘Open Circuit Voltage’. The OCV can be considered as the potential difference across the terminals of the cell when there is no net current flow. Under standard conditions, this is the ‘standard cell voltage’,  $V_r^\circ$ . When the fuel is hydrogen, the reversible voltage under standard conditions (STP) is 1.229V at 25°C [2].

## 1.2 Nernst Equation

The ‘Gibbs equation’ discussed in Section 1.1 has been highlighted the Gibbs free energy dependence with temperature. Nevertheless, this parameter is also affected of both reactant pressure and concentration. Consider, for example, a general reaction such as:



where x moles of A react with y moles of B to produce z moles of C. Each of the reactants, as well as the product, has an associated ‘activity’ (is a measure of the ‘effective concentration’ of a species in a reacting system) which is defined by the symbol  $a$ . Therefore,  $a_A$  and  $a_B$  represent the activities of the respective reactants, and  $a_C$  the activity of the product. If the case of gases behave as ‘ideal gases, the activity of this components in the system can be considered to be proportional to partial pressure (1.12).

$$a_x = \frac{Px}{P^\circ} \quad (1.12)$$

The activities of the reactants and products modify the Gibbs free energy change of a reaction. By using thermodynamic principles, for a chemical reaction such as the general example given in equation (1.13), the following holds:

$$\Delta\bar{g}_f = \Delta\bar{g}_f^\circ - RT \cdot \ln \left[ \frac{a_A^j * a_B^k}{a_C^m} \right] \quad (1.13)$$

where  $\Delta\bar{g}_f^\circ$  is the standard free energy change for the reaction.

Finally substituting  $\Delta\bar{g}_f^\circ$  into equation (1.10) it is possible to write the Nernst potential of the cell, known as the minimum voltage gradient that must be applied across the electrodes of the cell to have the electrolysis reaction.

$$V_r = \frac{-\Delta\bar{g}_f^\circ}{2F} - \frac{RT}{2F} \cdot \ln \left[ \frac{a_A^j a_B^k}{a_C^m} \right] \quad (1.14)$$

The Nernst equation can be used to analyse the influence of different parameters on the operation and/or performance of a fuel cell. For example, in reaction:



By substituting the activities of reactants and products with the relation (1.12), the Nernst equation will be:

$$V_r = V_r^\circ + \frac{RT}{2F} \cdot \ln \left[ \frac{a_{H_2} \cdot a_{O_2}^{1/2}}{a_{H_2O}} \right] \quad (1.16)$$

The first term on the right-hand side of equation (1.16) shows the effect of the temperature on the cell voltage while the second term shows the effect of the pressures of the reactants and product on cell voltage. The irreversibility in the voltage drop is accounted by the third term of the equation and is expressed by the activation, ohmic, concentration overpotentials.

In addition for a better analysis internal current and fuel crossover losses are evaluated. Finally, the generic equation of polarization curve for the electrochemical cell can be rewritten as:

$$V_r = \pm \frac{\Delta g_{reac}(T, p_i)}{ZF} \pm [\Delta V_{act}(i) + \Delta V_{ohm}(i) + \Delta V_{conc}(i) + \Delta V_n(i)] \quad (1.17)$$

The equation (1.17) underline the strongly dependence of current density ( $i$ ) in the voltage output of the fuel cell.

In the figure 1.3 an graphical representation of the polarization curve is showed:

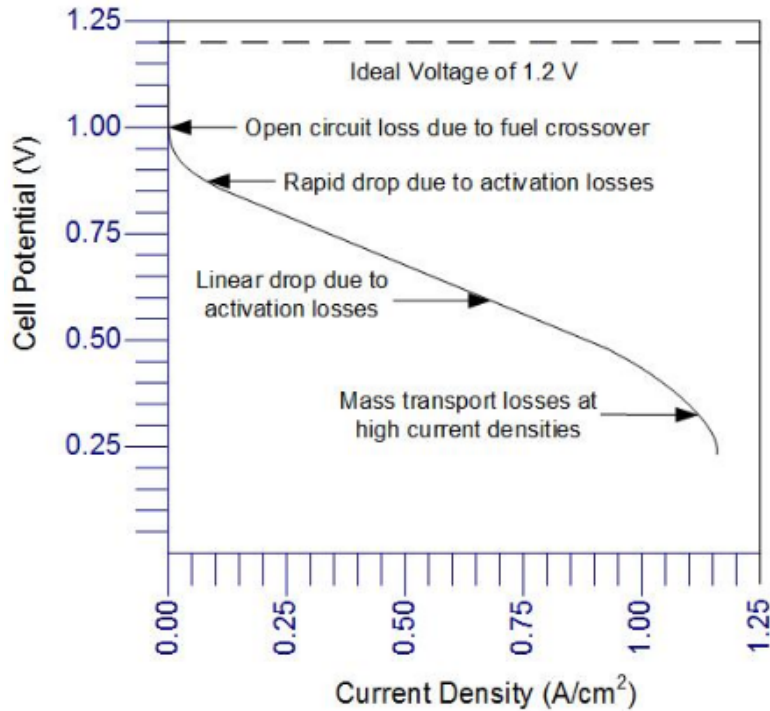


Figure 1.3: Polarization curve [2]

### 1.2.1 Fuel-cell Irreversibilities

The characteristic shape of the voltage versus current density relationships shown in figure 1.3 is the result of four major irreversibilities. The voltage losses which follow will be analyzed briefly here before being considered in more detail later, namely:

1. *Activation losses.* Depend on the slowness of the chemical reactions taking place on the electrodes surface. A part of the voltage generated is lost in driving the chemical reaction in moves the electrons to or from the electrode. The final effect on the polarization curve is strongly non-linear.
2. *Internal currents and fuel crossover.* This voltage loss results from a small amount of fuel moving through the electrolyte from the anode to the cathode (fuel crossover) and from electron conduction through the electrolyte (internal currents).  
Generally, the fuel loss and internal currents are both small, and thereby the net effect is usually not very important.
3. *Ohmic losses.* This voltage loss is proportional with the resistance of electrons flow through the electrodes, interconnections, as well as the resistance

to the flow of ions through the electrolyte. The effect in polarization curve is essentially linear.

4. *Concentration or mass-transport losses.* These losses in voltage are determined from the change in concentration of the reactants at the surface of the electrodes during the operation when the fuel is consumed.

The four categories of irreversibility are considered, in turn, in the following sections.

## 1.2.2 Activation Overpotential

The activation loss ( $\Delta V_{act}$ ) can be expressed with a general formula:

$$\Delta V_{act} = V - V_{eq} \quad (1.18)$$

where  $V$  is the measured electrode potential and  $V_{eq}$  is the theoretical equilibrium electrode potential. Going more in depth, the variation in potential at the surface of the electrode is similar for a great variety of electrochemical reactions.

This general behaviour can be expressed by the equation below.

$$\Delta V_{act} = A \ln \left( \frac{i}{i_0} \right) \quad (1.19)$$

where  $A$  is a constant, commonly referred to as the ‘Tafel slope’,  $i$  is the current density and  $i_0$  is the ‘exchange-current density’.

For a hydrogen fuel cell, the constant  $A$  in equation (1.19) is given by:

$$A = \frac{RT}{2\alpha F} \quad (1.20)$$

Where  $R$  is the universal gas constant and  $T$ , is the temperature in Kelvin (K). The parameter  $\alpha$  is called the ‘charge-transfer coefficient’ and is the proportion of the electrical energy applied that is harnessed in changing the rate of an electrochemical reaction. For the hydrogen electrode,  $\alpha$  is about 0.5 for a wide variety of electrode materials.

Regarding exchange-current density  $i_0$  can be visualized as follows. The reaction at the oxygen electrode of a proton-exchange membrane or acid electrolyte fuel cell is:



At zero current density the reaction is occurring, but the reverse reaction is also proceeding at the same rate. There is an equilibrium, which is expressed as:



Thus, there is a continual backwards and forwards flow of electrons from and to the electrolyte that constitutes the exchange-current density,  $i_o$ . The exchange-current density is crucial in controlling the performance of a fuel-cell electrode, in fact the differences in values of  $i_o$  between the two electrodes reflect the different rates of the reactions that take place on either side of the cell [2]. The Equation (1.19) and (1.20) can be rearranged to describe the cell current as a function of voltage. This is achieved by converting from the logarithmic to the exponential form, to give the Butler–Volmer equation:

$$i = i_o \left[ \exp \frac{n\alpha_a FV_{act}}{RT} - \exp \frac{-n\alpha_c FV_{act}}{RT} \right] \quad (1.23)$$

Where  $n$  is the number of electrons transferred in the electrochemical reaction and  $\alpha_a$  and  $\alpha_c$  are the charge-transfer coefficients at the negative and positive electrodes, respectively.

The Butler–Volmer equation expresses the current produced by an electrochemical reaction in terms of the rates of reactions at the two electrodes.

By increasing the current density it is possible to improve the fuel-cell performance, this can be fulfilled in various ways:

- Raising the cell temperature.
- Using more effective catalysts.
- Increases the real surface area through the creation of roughness on the electrodes.
- Increasing reactant concentration, by substituting the air with pure oxygen. With this action the catalyst sites will be more effectively occupied by reactants.
- Increasing the system pressure.

When  $\alpha=0.5$ , the equation can be rewritten implementing the hyperbolic sine:

$$i = 2i_o \sinh \left( \frac{n_e FV_{act}}{2RT} \right) \quad (1.24)$$

Isolating the activation overpotential the final equation become:

$$\Delta V_{act} = \frac{2RT}{n_e F} \sinh^{-1} \left( \frac{i}{2i_0} \right) \quad (1.25)$$

### 1.2.3 Internal current and fuel Crossover

The internal currents losses are generated by conduction of electrons, the resulting reduction in voltage is relatively small

The fuel crossover, instead is more important, is related to the possibility to have a migration of hydrogen from the anode, through the electrolyte, to the cathode. The hydrogen will react directly with oxygen on the cathode catalyst to be consumed and thereby generate no current from the cell. The previously mentioned two negative effects are essentially comparable and can be take into account with a single parameter named internal current density ( $i_n$ ). Considering for simplicity a system with a voltage drop only determined by the ‘activation overpotential’ at the cathode, then the cell voltage ( $V_c$ ) will be reduced only by the amount given by equation (1.26):

$$\Delta V_n = V_r - A \ln \left( \frac{i + i_n}{i_o} \right) \quad (1.26)$$

### 1.2.4 Ohmic Overpotential

The resistances to the flow of ions in the electrolyte and of electrons through the electrode material are included in the Ohmic losses. Because the ionic flow in the electrolyte obeys Ohm’s law [7], the ohmic losses can be expressed by the equation:

$$\Delta V_{ohm} = i \cdot r \quad (1.27)$$

Where  $r$  represents the ‘area specific resistance’ (ASR) The ‘ohmic loss’ of voltage is significant in all types of cell and is especially important in the case of the SOFC. Three ways of reducing the internal resistance of a cell are as follows:

- Using electrodes with the highest possible conductivity.
- Making the electrolyte as thin as possible. Unfortunately, this approach is often difficult, a good compromise is always needed. The electrolyte can be very thin but still must have adequate thickness to prevent internal shorting between electrodes [2]. It is important to underline that the behavior of the high temperature cells is mainly represented by the area specific resistance.

### 1.2.5 Mass transport losses

The rate of mass transport to the reaction sites in a porous electrode of a fuel cell can be described by the diffusion of gases in the pores. The gases have to spread through the gas filled pores of the electrode in order to reach the reaction sites.

The concentration polarization become significant increasing the current rate, this implies a reduction in gas partial pressure at the reaction sites respect the bulk one. Diffusion through the porous material is typically described by either ordinary or Knudsen diffusion.

For Knudsen diffusion, molecules collide more frequently with the pore walls than with other molecules. Upon collision, the atoms are instantly adsorbed on to the surface and are then desorbed in a diffusive manner.

As a result of frequent collisions with the wall of the pore, the transport of the molecule is impeded [8]. For this reason to account for the tortuous path of the molecule rather than along the radial direction, an effective Knudsen diffusion coefficient may be use:

$$D_{eff} = \frac{\varepsilon}{\tau} \cdot D_{bulk} \quad (1.28)$$

- $D_{eff}$  is the effective diffusion coefficient.
- $D_{bulk}$  is the diffusion in bulk condition (in the gas channel side).
- $\varepsilon$  is the porosity of solid matrix composing the electrode, more pores means high diffusion but at same time lower mechanical stability.
- $\tau$  is related to the tortuosity of the electrode, an higher tortuosity means a lower possibility of molecule to diffuse inside the porous structure.

Finally the voltage drop caused by the consumption of the fuel gas can be calculated as the difference in concentration between bulk and catalyst side, which leads to the following equation:

$$\Delta V_{conc} = B \ln \left( 1 - \frac{i}{i_l} \right) \quad (1.29)$$

Where  $i_l$  is the current density limit and it is related to the mass transport capability, and B is equal to:

$$B = \frac{RT}{ZF} \quad (1.30)$$

### 1.2.6 Combining the Irreversibilities

It is useful to construct an equation that brings together all the irreversibilities associated with fuel cells:

$$V_c = V_r - (i + i_n)r - A \ln \left( \frac{i + i_n}{i_o} \right) + B \ln \left( 1 - \frac{i + i_n}{i_l} \right) \quad (1.31)$$

where

- $V_r$  is the reversible open-circuit voltage.
- $i_n$  is the sum current density equivalent of fuel crossover and the internal current density.
- $A$  is the slope of the Tafel line.
- $B$  is the parameter used in the mass-transfer overvoltage equation.
- $i_l$  is the limiting current density at the electrode that has the lowest one.
- $r$  is the ASR
- $i_o$  is either the exchange-current density.

## 1.3 High temperature electrolysis

High Temperature Steam Electrolysis (HTSE) is a unique technology for hydrogen production in which the electrolysis reaction is carried out at high temperatures ranging from 700 to 1000 °C [9]. The main motivation for HTSE lies in its potential for decreasing the electricity demand compared to electrolysis at low temperature (alkaline and PEM electrolysis) as explained in the equation (1.32).

$$W_{el} = \Delta H - T_{cell}\Delta S = \Delta G \quad (1.32)$$

In which  $\Delta G$  (Gibbs free energy) represents the minimum electricity required by the electrolysis reaction,  $T_{cell}\Delta S$  (where 'S' is entropy and 'T' cell temperature) represents the heat required by the reaction and finally  $\Delta G$  is the energy required so that the reaction occurs.

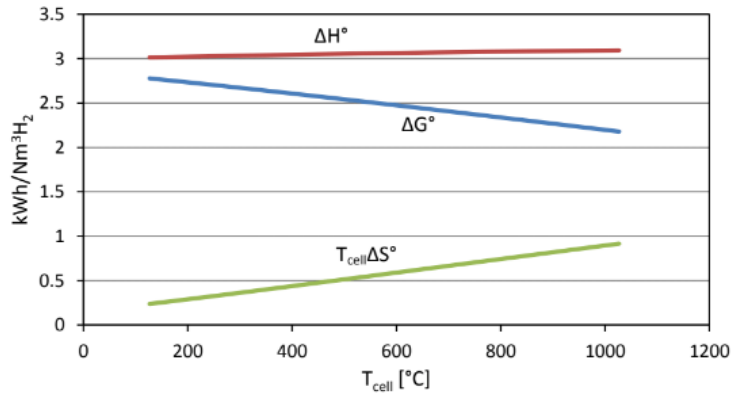


Figure 1.4: Steam electrolysis ideal energy requirement

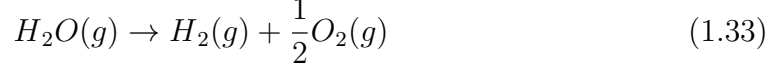
The figure 1.4 shows that at high temperature, the thermodynamic conditions of the electrolysis reaction are more favourable, this because the molar Gibbs energy of the reaction ( $\Delta G$ ) decreases with temperature while the molar enthalpy of the reaction ( $\Delta H$ ) remains essentially unchanged, while the opposite happen for the product entropy temperature. Another advantage of the high temperature operation is related to the kinetic reaction improvement, for this reason differently from low temperature fuel cells, the precious metal electrocatalysts are not more necessary. Through the substitution of a portion of electricity input to the SOEC with heat may offer the possibility of obtaining higher efficiencies, and consequently lower costs and GHG emissions compared with alkaline and PEM electrolysis [10]. Another advantage of HTSE (and electrolysis in general) is production of pure hydrogen without the need for hydrogen purification units that are required in SMR (Pressure Swing Adsorption e PSA, amine CO<sub>2</sub> removal). This may be beneficial both in terms of cost and size of the hydrogen production plant. However, there are several technical (e.g., SOEC lifetime), and manufacturing issues (e.g., materials that can withstand the high temperatures of HTSE) that must be resolved before this technology can become a viable alternative for SMR [11].

### 1.3.1 Solid oxide electrolytic cell

The key components of an SOEC are a dense ionic conducting electrolyte and two porous electrodes. The fundamental mechanisms involved in SOEC operation are shown in figure 1.5.

Steam is fed to the porous cathode. When required electrical potential is applied to the SOEC, water molecules diffuse to the reaction sites and are dissociated to form hydrogen gas and oxygen ions at the cathode–electrolyte interface. The oxygen ions are transported through the dense electrolyte to the anode. The hydrogen gas produced diffuses to the cathode surface and gets collected. On the anode side,

the oxygen ions are oxidized to oxygen gas and the produced oxygen is transported through the pores of the anode to the anode surface [12]. The net reaction of SOEC is the opposite of the SOFC:



Instead for what concern the half reaction in the anode and cathode respectively:

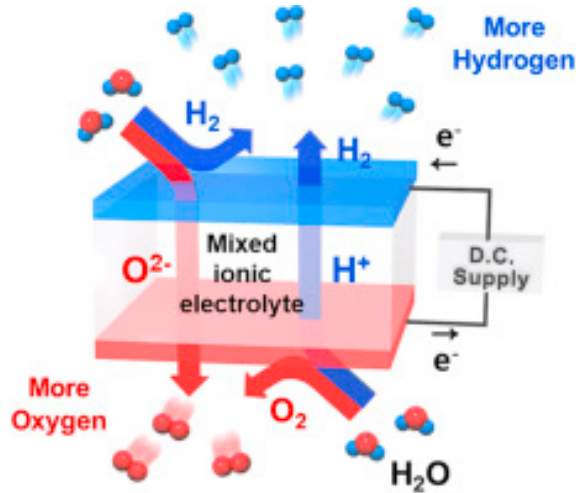


Figure 1.5: Schematic of SOEC Hydrogen production [13].

As mentioned before, the SOEC and SOFC systems operate at high temperature, for this reason the components must meet certain requirements for efficient and cost-effective operation. The SOEC/SOFC requirements which follow will be analyzed briefly here before being considered in more detail in 'state of art section':

- The dense electrolyte should be chemically stable and have good ionic conductivity with low electronic conduction to achieve high energy conversion efficiency.

- The dense electrolyte must be gastight to avoid any possibility of recombination of fuel reactant  $H_2$  and  $O_2$ , but at same time it should be very thin to minimize the ohmic overpotential losses.
- Both electrodes should have suitable porosity and pore size to support gas diffusion between the electrode surface and the electrode–electrolyte interface and provide sufficient reaction site.
- The interconnect materials must be chemically stable in the reducing/oxidizing environments at high temperature and a very good electronic conductor.
- The thermal expansion coefficients of both electrodes should match to that of the electrolyte to prevent material failure of the electrolyte due to high mechanical stress.
- The cost of the component materials and the manufacturing cost should be as low as possible.

Researches are concentrated during the years on finding a combination of materials that satisfies these requirements.

## 1.4 State of art

The solid oxide fuel/electrolytic cell are completely solid-state device that operates with oxide ion-conducting ceramic material as the electrolyte. Beyond the benefits mentioned above, the high temperature operation means that precious metal electrocatalysts are not necessary, consequently, the SOFC can accept a wide range of converted (reformed) fuels, which include coal-derived gases. In this perspective for example, both hydrogen and carbon monoxide (CO) can serve as fuels the same SOFC, as shown in Fig 1.6,1.7.

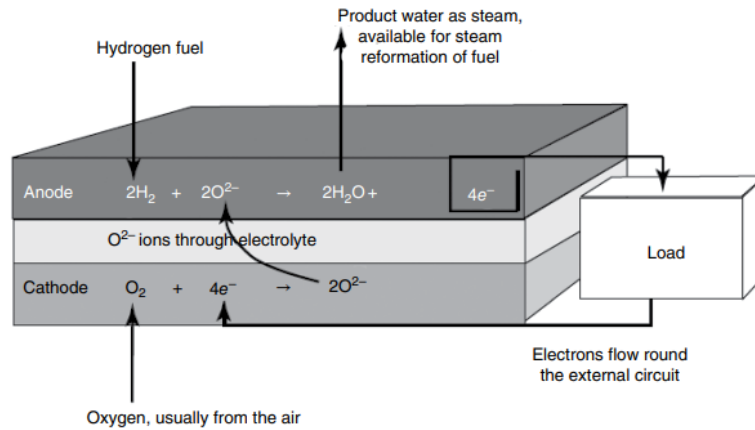


Figure 1.6: Anode and cathode reaction for SOFC, using both hydrogen fuel [2]

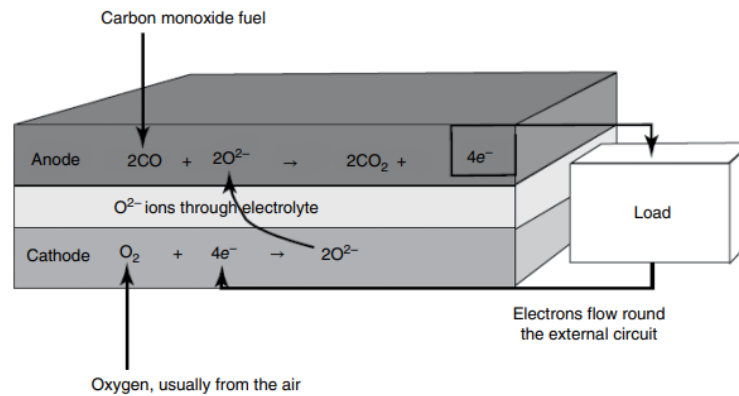


Figure 1.7: Anode and cathode reaction for SOFC, using carbon monoxide fuel [2]

Until recent years, all SOFCs/SOECs have been based on an electrolyte of zirconia stabilized with the addition of a small percentage of yttria ( $\text{Y}_2\text{O}_3$ ).

The zirconia problem is that it becomes a oxygen ions ( $\text{O}_2^-$ ) conductor only above a temperature of about  $700^\circ\text{C}$ .

This is the highest operating temperature range of all fuel cells and thereby presents extra challenges in terms of construction and durability.

Besides the negative aspects the solid oxide fuel cells typically exhibit very good electrical efficiencies (around 50%).

The anode is usually a cermet (composite material composed of ceramic and metallic materials) of yttria-stabilized zirconia (YSZ) and nickel. The nickel is chosen principally because it has a good electronic conductivity and is resilient under chemically reducing conditions. Moreover, as mentioned in the section before it is also more sulfur resistant than the precious metal catalysts employed in low-temperature fuel

cells.

In terms of cathode, most of them are made from electronically conducting oxides or a ceramic material that possesses both ionic and electronic conductivities [2]. The currently used material of the latter type is strontium-doped lanthanum manganite (LSM),  $La_{1-x}Sr_xMnO_3$  (fig1.8).

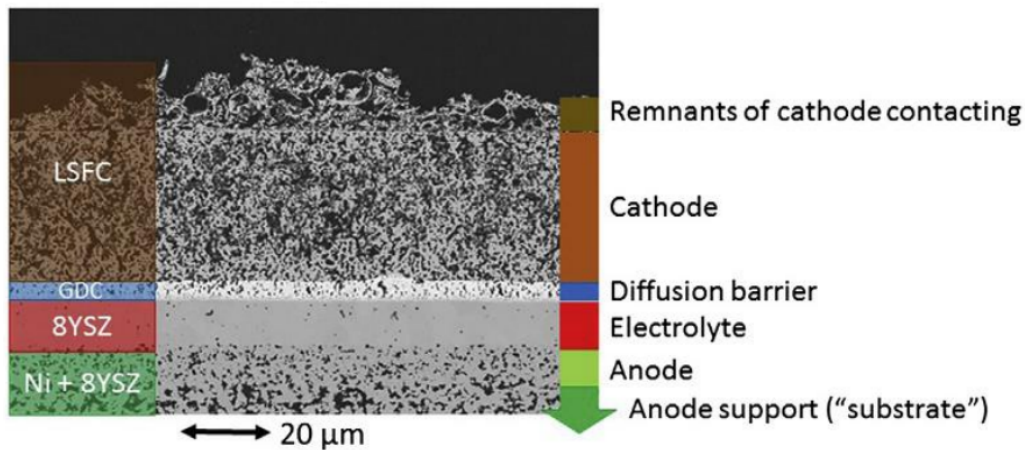


Figure 1.8: Anode supported cell state of art

### 1.4.1 Electrolyte

In an SOFC, the electrolyte is exposed at high temperatures to both oxidizing (air side) and reducing (fuel side) atmospheres. For this reason, to succeed in long-term SOFC/SOEC operation the electrolyte requires to have the following properties:

- A dense structure, impermeable to gas.
- Sufficient ionic conductivity to minimize ohmic loss.
- Chemical stability, in both oxidation and reduction processes.
- The thermal expansion coefficients, must match at the interfaces and mechanical compatibility with both electrodes.

Zirconia doped with 8–10 mol.% yttria (YSZ) continues to be the most effective electrolyte for HT-SOFCs although several other materials have been investigated. Pure zirconium dioxide ( $ZrO_2$ ) has a monoclinic crystal structure and at room temperature is a scarce ionic conductor.

When heated above 1170 °C, it undergoes a phase transformation from monoclinic

to tetragonal and then, by a further increasing in temperature to 2370°C, it modifies to a cubic fluorite structure.

In order to stabilize the cubic structure at lower temperatures and at same time to increase the concentration of oxygen vacancies, acceptor dopants are introduced into the cation sublattice.

Example dopants are  $Ca^{2+}$  and  $Y^{3+}$ , which produce calcia-stabilized zirconia (CSZ) and YSZ, respectively, as illustrated in fig 1.9. Each dopant stabilizes the cubic fluorite structure and improves the oxygen-ion conductivity of the zirconia [2].

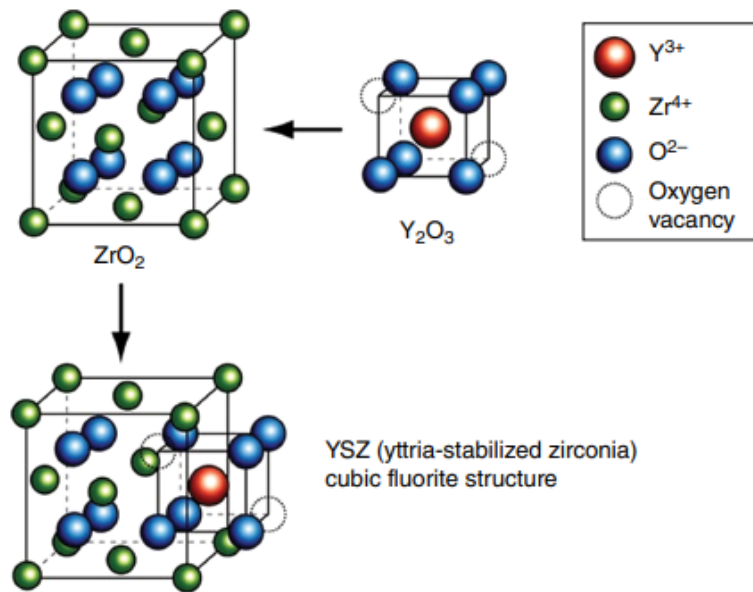


Figure 1.9: Structure of yttria-stabilized zirconia [2]

Zirconia presents a very good chemical stability in both reducing and oxidizing environments, at the anode and cathode regions.

The replacement of some  $Ca^{2+}$  ions with  $Y^{3+}$  ions in the fluorite structure, allows the  $O^{2-}$  ions conduction.

## 1.4.2 Anode

In the nickel–YSZ cermet that forms the anode of state-of-the-art HT-SOFCs. The nickel (At least 30 vol.%) is typically used in the cermet in order to maintain a right porosity so that mass transport of reactant and product gases is not compromised while offering a proper electronic conductivity.

The porous YSZ serves to block the coarsening of the metal particles and provides the anode with a thermal expansion coefficient similar to that of the electrolyte.

Nickel and YSZ are not miscible and non-reactive in each other over a wide range of temperature. Both these properties promote the manufacturing of YSZ cermets and ensure the preparation through NiO and YSZ powders (sintering process).

Reduction of NiO to Ni in situ leads to a highly porous (20–40%) YSZ structure that contains connected Ni particles on the surface of the YSZ pores [2]. The active reaction sites, typically called the triple-phase boundary (TPB) where the electronic, ionic, and gas phase coexist are located in the intersection between pores structure and nickel-zirconia particles.

### 1.4.3 Cathode

Despite is not so chemically stable with YSZ, strontium-doped LSM has received lots of attention recently, becoming the most widely used cathode material for the SOFC for both HT- and LT-SOFCs. The LSM belongs to the family of perovskite. They have a crystal structure represented by the general formula  $ABO_3$ , where an A-site ion on the corners of the lattice is usually an alkaline earth or a rare-earth element and the B-site ions in the centre of the lattice are transition metal elements. Either the A or B cation can be substituted by introducing other cations of the same or different valency.

As with many perovskites, the crystal structure of LSM undergoes a phase change from an orthorhombic structure at room temperature to a rhombohedral form above 600°C, this transition enhance the piezoelectric properties. The mixed ionic–electronic conductivity of LSM can be improved by substituting some of the A-sites with  $Sr_2^+$ . It is particularly notable that the applied partial pressure of oxygen affect the LSM structure and oxygen non-stoichiometry. The material is stable over large range of oxygen partial pressures, but at very low levels, it can dissociate to form two phases, namely,  $La_2O$  and  $M_nO$  [2].

### 1.4.4 Interconnect material

When the cell operate at medium temperature (around 800 C°), it is possible to use oxidation-resistant metallic alloys for the interconnects. Ferritic steels are currently the most common option. Compared with lanthanum chromite ceramic, this metallic alloys offer advantages such as improved manufacturability, significantly lower fabrication costs and advanced thermal and electrical conductivity.

Alloys, such as Crofer22 APU (a high-temperature ferritic stainless steel), have been engineered produced with thermal expansion coefficients in order to match those of SOFC ceramic components.

Unfortunately, the chromium, under high oxygen partial pressure at the cathode vapourize and deposit at the LSM–YSZ three-phase boundary causing permanent deterioration.

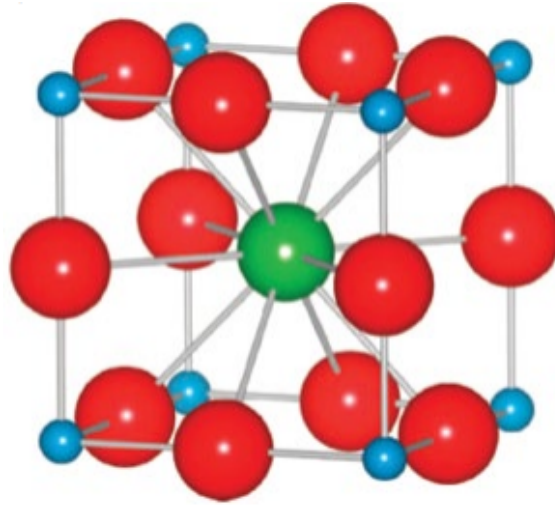


Figure 1.10: Cubic perovskite structure representation [2].

The vaporisation of chromium from the metallic interconnect can lead to important degradation of the SOFC electrical properties. Recent studies focus on the use of  $(Mn,Co)_3O_4$  spinels, due to their excellent electrical properties and the compatibility of coefficient of thermal expansion (CTE) with ferritic stainless steel. The spinel coatings provide sufficiently low ASR values [14].

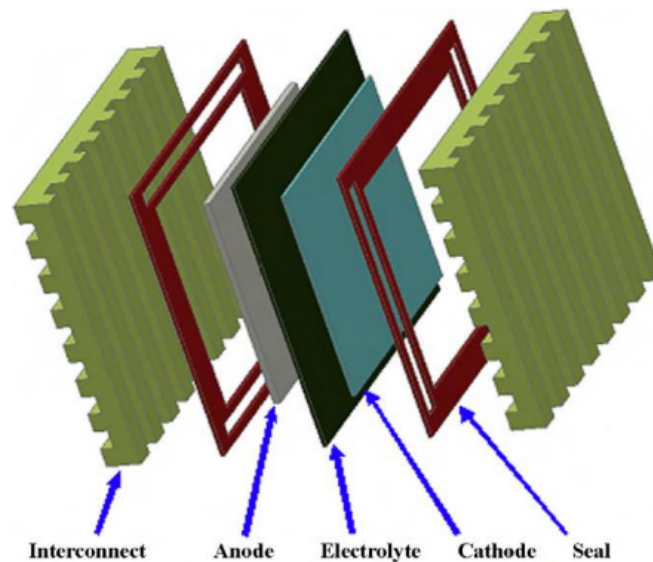


Figure 1.11: Cell structure [15].

### 1.4.5 Sealing materials

A key issue with SOFCs, in particular for planar layout, is the sealing between metal and ceramic components to achieve gas tightness.

The seal needs to be chemically and thermally stable and compatible with the cell component materials.

The most common practice has been the glasses use, which soften as the cells are heated up above the glass transition temperature and form a seal all around the cell, this because by carefully choosing the composition, they meet most of the requirements of an ideal sealant, with the difference that the glass ceramic have much higher stability than the simple glass [16]. Glass seals are used in planar stack designs in which with only one layer may be assembled several cells.

A peculiar problem connected with the use of glass seals is the migration of silica from the glass at high temperature, particularly onto the anodes which leads to a strongly deterioration in cell performance. Glass ceramics have been adopted for all-ceramic stacks, but migration of the silica component can still be a problem on both the anode and cathode sides [2].

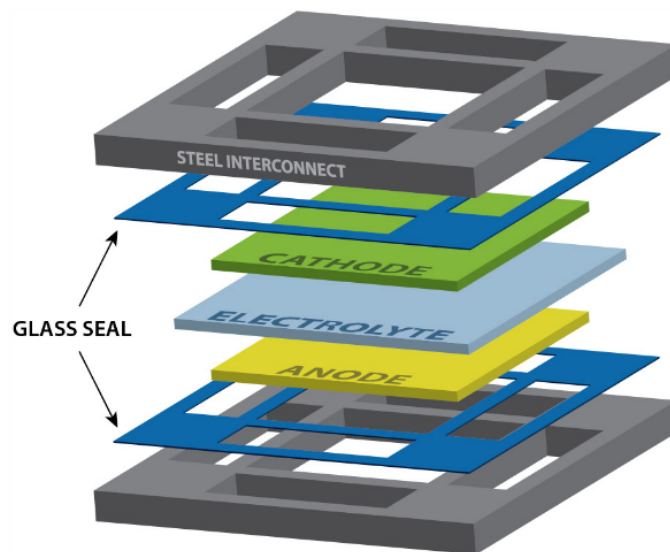


Figure 1.12: Glass Sealing material [17]

# Chapter 2

## Test bench experimental setup

For the analysis of a planar solid oxide cell a test bench is designed. The present test station is composed by:

- A Gas Distribution System, to feeds the cell with different gases.
- A Controlled Evaporator Mixer (CEM), used for humidify and heat up the incoming fluids.
- Electric auxiliaries.
- Housing and test cell.
- A data acquisition and control system which can be controlled manually, through a software installed in a local PC, or remotely.

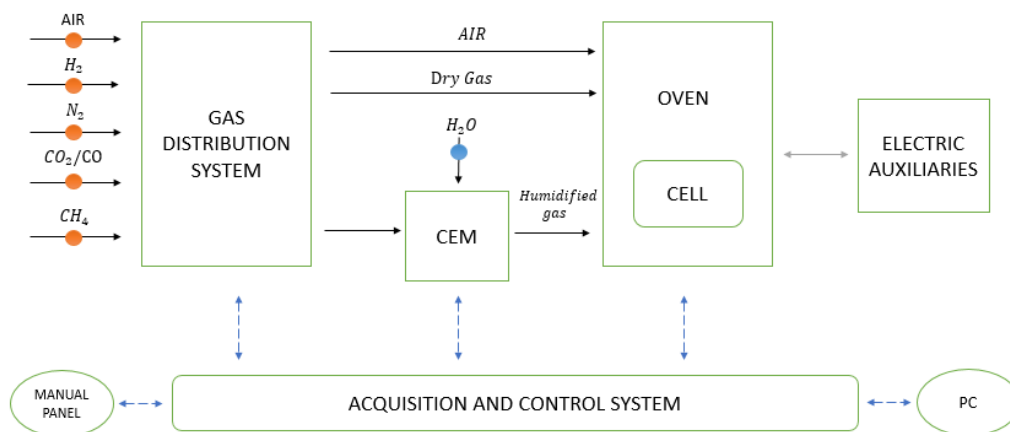


Figure 2.1: Schematic block diagram indicating the main subsystems.

The figure 2.1 indicates the main subsystems involved in the test bench. In particular the solid black lines point out the mass fluxes, the solid grey line the energy fluxes, and the dashed lines the data exchanged between subsystems. In addition, the red circles highlighted in figure 2.1 represent the mass flow controllers present in the gas distribution system, instead the blue circle the liquid flow meter.

## 2.1 Gas distribution system

The gas distribution system connects the test bench with the laboratory gas storage tanks. The system is composed by valves, pipes and mass flow controllers (Bronkhorst). Mass flow controllers are monitored and controlled by the acquisition and control system through an internal electric actuator.

Manual valves are located before and after each mass flow controllers, allowing the isolation of them. In addition filters are used to avoid any impurities entering in test cell.

The test bench gas / steam circuit is composed by 2 main lines: one called 'anode line' which is used to generate a mixture of gas ( $H_2$ ,  $CO_2$ ,  $CO$ ,  $N_2$ ,  $CH_4$ ) and water vapor and guide it to the test cell in the Oven system, and the other one 'catode line' which is used to provide air to the fuel cell cathode (SOFC operation)..

The gas mixture is generated by gas lines present in the laboratory (at 2.5 bar) and managed by mass flow controllers (MFCs).

In total nine MFCs are installed on the anode line and there is only one MFC on the catode line connected to the laboratory compressed air line, displayed in figure 2.2.

Each controller unit is designed for a specific gas and flow rate range, for example the maximum flow rate allowed is 2000 Nml. The gas lines are made of steel with Swagelok fittings (fig. 2.3).

### 2.1.1 Mass flow controller

The mass flow controllers used in the test bench belong to EL-FLOW Select series (Bronkhorst) Mass Flow Meters and Controllers (fig.2.4). These series of instruments can withstand a operative pressure up to 400 bar. The specific mass-flow meters selected for the bench operates at near-ambient pressure (maximum tolerable pressure 8 bar) and 0-2000 [Nml/min]. In addition the EL-FLOW Select series are equipped with a digital pc-board, offering high accuracy, excellent temperature stability and fast response (500 msec).

The main digital pc-board contains all of the general functions needed for measurement and control. In addition to the standard RS232 output the instruments also



Figure 2.2: Gas distribution connection



Figure 2.3: Swagelok fitting

offer analog I/O. Furthermore, an integrated interface board provides DeviceNet, CANopen, PROFIBUS®DP, Modbus, FLOW-BUS, EtherCAT®, PROFINET, Modbus/TCP or EtherNet/IP protocols [18].



Figure 2.4: The EL-FLOW Select series Mass Flow Meters and Controllers for gas applications [18].

#### 2.1.1.1 Working principle

The heart of the thermal mass flow meter/controller is the sensor, that consists of a stainless steel capillary tube with resistance thermometer elements.

The gas flows through the bypass sensor is warmed up by heating elements. Consequently the measured temperature difference between  $T_1$  and  $T_2$  is directly proportional to mass flow through the sensor.

In the main channel Bronkhorst applies a patented laminar flow element consisting of a stack of stainless steel discs with precision-etched flow channels [18].

Thanks to the perfect flow-split the sensor output is proportional to the total mass flow rate (fig.2.5).

For what concern the control valve, it is a proportional, electro-magnetic control valve with extremely fast and smooth control characteristics.

With reference to the specific field of application there are different series of them; there is a standard direct acting valve for common applications, a pilot operated valve for high flow rates [18].

The case study considered in this work falls within the low flow rates applications.

#### 2.1.2 Risks Analysis for an explosive environment

Working with dangerous substances, an analysis was carried out of the risks of forming an explosive atmosphere due to the emission of gases, vapors. The emission sources considered are essentially constituted by the valves of gas interception. The

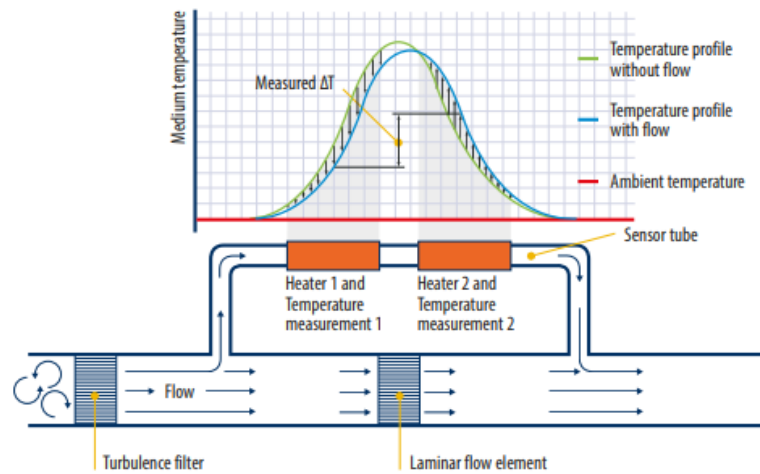


Figure 2.5: Mass flow controller working principle [18].

emission sources are of second degree (infrequent emission and for short periods), only in case of failure of the component and wear.

The test bench dangerous areas are represented below through cones pointing upwards. The cones size define the hazard distance (fig. 2.6).

## 2.2 CEM

The gas path in the anode line of the mass flow controller panel flows into a three-way valve. Depending on the position of the valve, the flow can be direct towards the hood (VENT position), or towards the test cell (CEL position). In the 'CEL' direction the circuit is divided into two new ramifications: humidification by means of CEM, or dry gas. The Controlled Evaporation and Mixing (CEM) System humidifies using a flow of liquid water supplied by a liquid mass flow meter. The liquid water flow is then mixed with a dry gas flow, which acts as a carrier and transports the liquid flow to the evaporator-mixer. The two components are connected via power and communication cables (fig. 2.7,2.8). Piping exiting from CEM is maintained at 120 °C, in order to avoid water condensation.

For what concerns the cathode side (air line), there is only one line controlled by the MFC5.

The air flows through two 3-way valves where it can be directed to the hood or the cell.

If the air flows in the cell direction, a Svagelok connection links the cathode input of the test cell with the entering fresh stream.

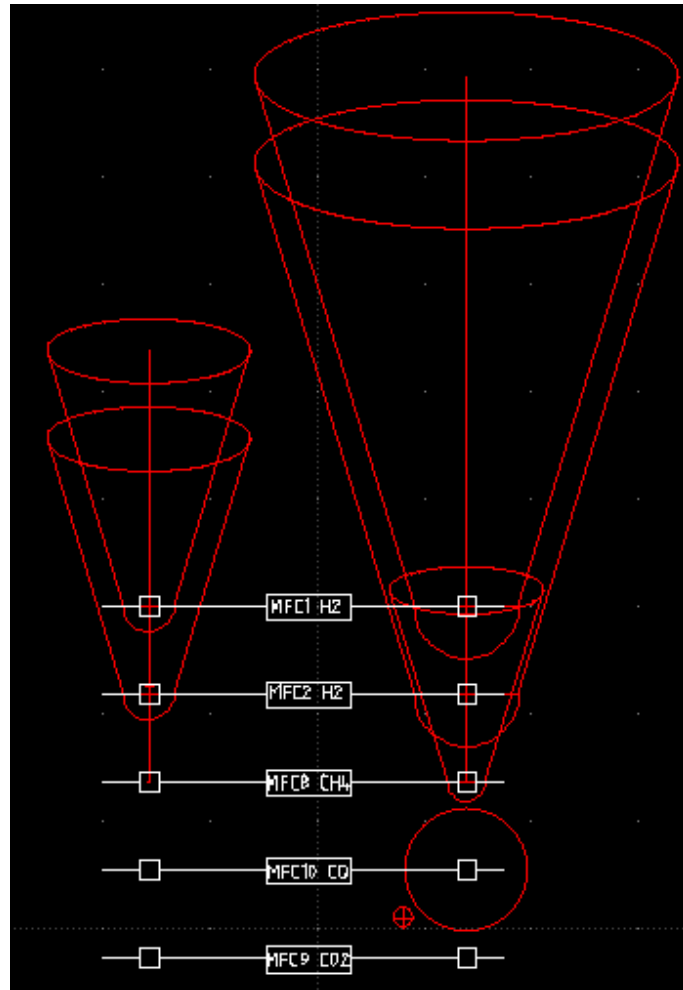


Figure 2.6: Danger cones

### 2.2.1 CEM working principle

At room temperature the liquid (precursor fluid for humidification purposes) is drawn from a line of demineralized water under pressure directly connected with a liquid flow controller.

The required flow rate is controlled to the setpoint value by a control valve (C) forming an integral part of the patented liquid flow and carrier gas mixing valve (M). The formed mixture is subsequently led into the evaporator to achieve total evaporation (E) [19]. The CEM working principle is displayed in figure 2.9.

The CEM-system is ideally suited to the accurate adjustment of moisture, which can be controlled with great flexibility, maintaining a very high stability.

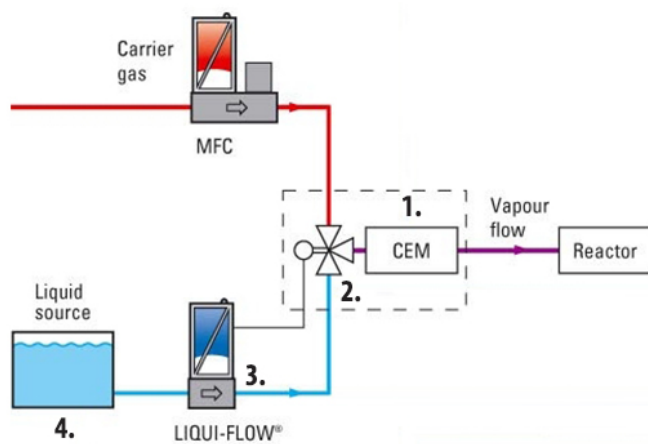


Figure 2.7: CEM connection.



Figure 2.8: CEM connection with liquid flow meter.

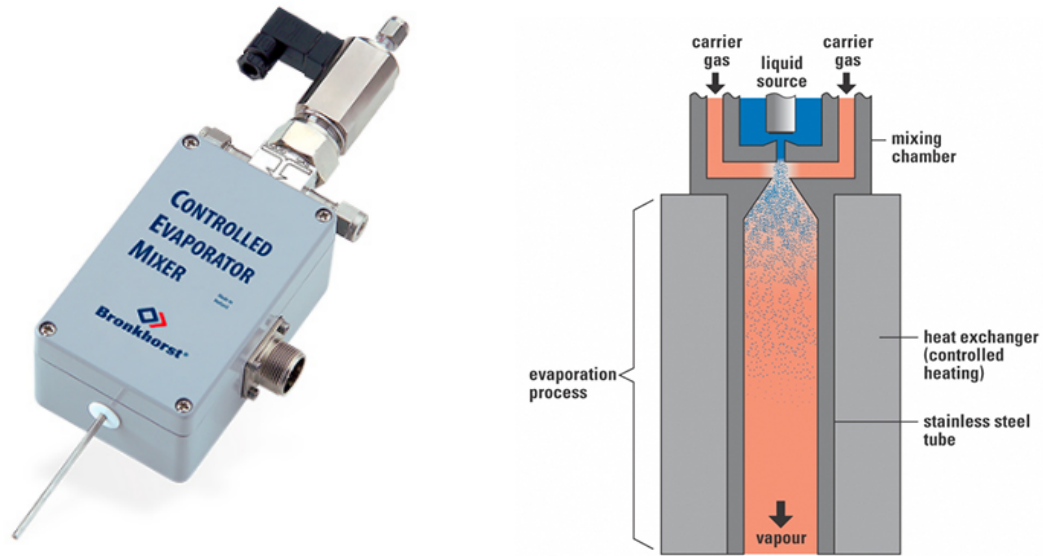


Figure 2.9: CEM working principle [19].

## 2.3 Oven and test cell

The anode and cathode gas lines supply the test cell. To reach high and stable temperatures levels, the cell is placed in an oven heated by four resistances (fig. 2.10). The electric current supplied to the resistances is controlled by the acquisition and control system. The heated chamber is insulated from the external environment by walls made of removable refractory bricks, in addition a ceramic plate is added on the top of chamber in the way to thermally close the system.

To monitor the oven temperature, thermocouples are installed inside the four resistances. Due to thermal dispersions, in order to have the desired temperature in the center of the oven (eg  $800\text{ }^{\circ}\text{C}$ ) it is necessary to bring the resistances to a higher  $T$  ( $830\text{ }^{\circ}\text{C}$ ).

To control and read the temperature level inside the oven a Eurotherm system is used (fig.2.11).

### 2.3.1 Eurotherm

Eurotherm controllers will automatically control process variables such as temperature, humidity, pressure, for this reason they belongs to the 'automatic control loop'. It consists of a sensor to measure the temperature, a controller and a power regulator (fig. 2.12).

The controller compares the measured temperature with the desired temperature,

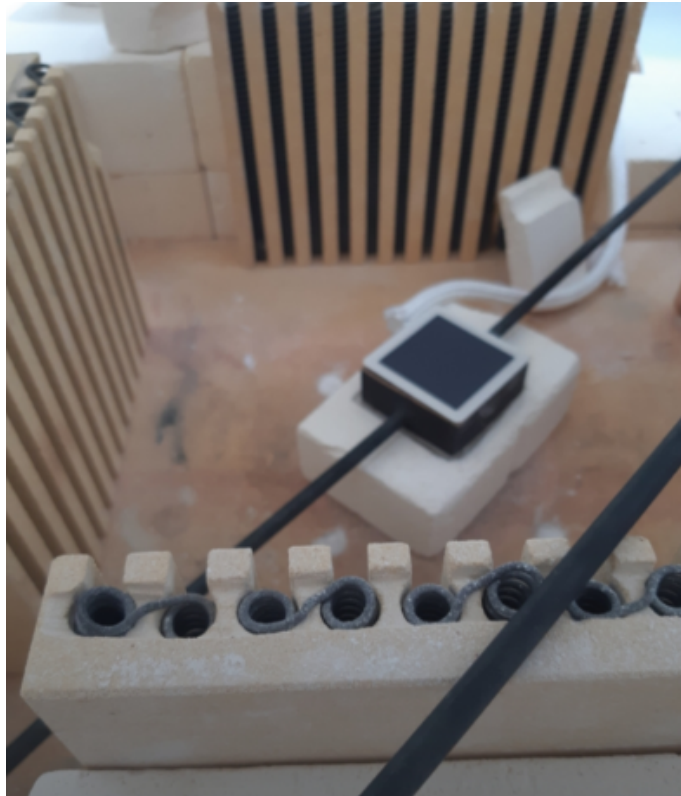


Figure 2.10: Cell placed in the oven



Figure 2.11: Eurotherm [20]

called the ‘setpoint’, and regulates the output power to make them the same [21]. The measured temperature is referred to as the ‘Process Value’.

The difference between the setpoint and the measured value is called the ‘error signal’. The automatic control loop aim is to reduce this error to 0.

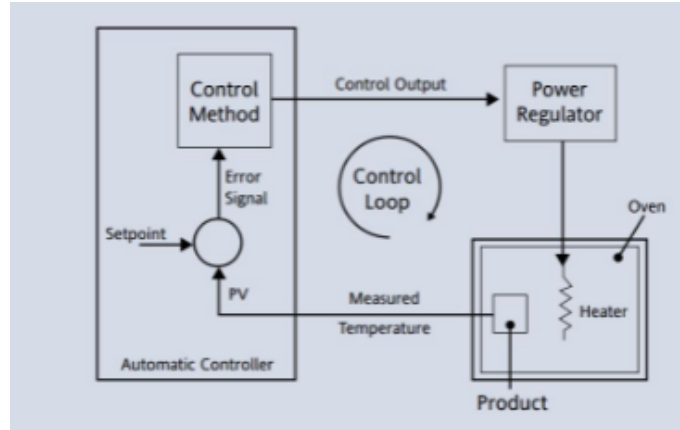


Figure 2.12: Automatic Control loop [21]

### 2.3.2 Test Housing

The housing consists of two parts that are in contact with the anode and cathode of the cell allowing:

- To distribute the gases through holes in the housing facades and to collect the products of the reaction.
- To conduct the current (being the metal a good electric driver).

The solid oxide cell behaves like a voltage generator of approximately 1 volt. It is electrical connected with the external electronic load through a circuit generated by the linkage between exhaust gases steel pipes coming out from the oven and twisted and pinched cables, as in fig.2.13.

As regards the assembly of the cell, for a better distribution of electric current, metal grids are inserted between the gas distribution base and the tested cell. Furthermore, a thin platinum cable is placed between the grids and the tested cell for voltage measurement (fig. 2.14).

The reactant gases mixture first flow into the anode side from the supply pipe and finally they are collected by the exhaust gas pipe at the cell outlet. Same thing happens to the cathode side with air, in addition the two flows (cathode line and anode) never mix.



Figure 2.13: Pipes connected with twisted cables.

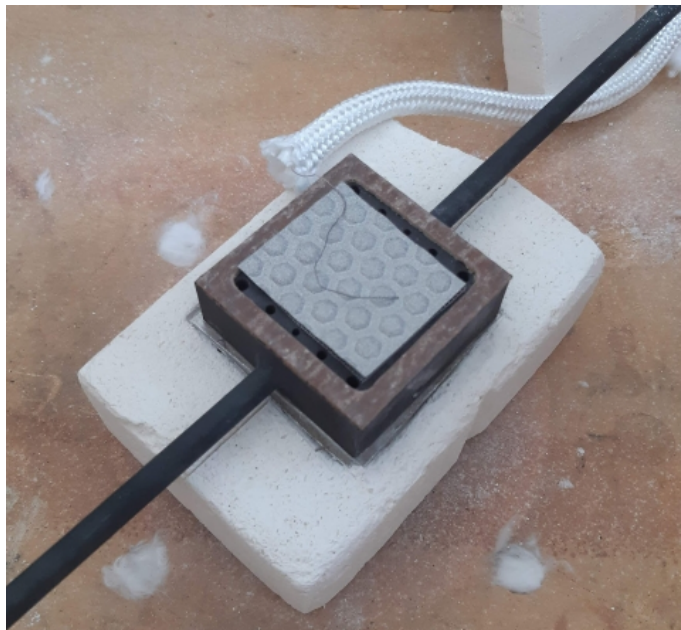


Figure 2.14: Representation of the metal grid, insulating frame and platinum wire for voltage measurement.

At the outlet, the two streams are taken to the suction hood, which should be equipped with sensors to control possible  $H_2$  and  $CO$  leakages.

## 2.4 Electric auxiliaries

The electric auxiliaries system is based on two electronic load:

- *Oven power supply*, controlled by the acquisition and control system in order

to supply a DC current to oven resistances, able to satisfy the temperature level imposed by the operator.

- *The cell electronic load*, controlled through the control software of user interface, it acts as a current generator imposing the current level in the tested cell.

Current wires are connected to the electronic load, while the voltage ones are connected to a terminal board from which the voltage signal is collected and carried to the data acquisition system. By inverting the cell-load circuit with a physical switch is possible to invert the wires connection between cell and load. This means that it is possible to have a switch between SOFC and SOEC modality without any particular change in the system (fig.2.15).

The figure 2.15 show the oven power supply, the cell electronic load and the additional supply (located in the lower position), and the SOEC/SOFC switch.

In the figure 2.16 below are displayed instead the SOFC and SOEC electronic circuits.

## 2.5 Acquisition and Control system

The last subsection is related to the acquisition and control system. The system is constituted by real-time monitoring and control system (CompactRIO, National Instruments), a Labview-based control software implemented in the CompactRIO and connected to a remote server for data storage and web-interface management, and finally a manual control panel (physical interface for MFCs, resistances, oven, eurotherm and electronic load). The test bench can be managed locally, with a computer connected to the CompactRIO or a manual control panel, or remotely.

### 2.5.1 Local software and hardware

The data signals coming from the thermocouples, MFC, CEM electronic loads and voltage probes are acquired by the CompactRIO, elaborated and sent to a control software installed to a server. The software receives all the signals and allows the user to insert set-point values which are: Oven temperature, cell current and voltage, gas and water flow rate.

Through the manual control panel (fig. 2.17) some of these variables can be set also manually ( mass flows, oven temperature), and gives the possibility to verify via panel screens the accuracy of the values acquired, The commands are generated by the deployment of advanced PID control algorithms.

### 2.5.1.1 PID control

PID control is also referred to as “Three-term” control. The three terms are:

- ‘P’ for *Proportional term*, it delivers an output which is proportional to the size of the error signal.  
If the controllers have only the proportional functionality, the physical quantity is controlled at setpoint with a certain offset error.
- ‘I’ for *Integral term*, it removes steady state control offsets by ramping the output up or down in proportion to the amplitude and duration of the error signal.
- ‘D’ for *Derivative term*, it is proportional to the rate of change of the temperature or process value. It is used in order to avoid overshoot and undershoot of the setpoint and to restore the process if there is a sudden change in demand [21].

The output of the controller is the sum of the above three terms.

### 2.5.2 Development of ‘remote lab’ concept

The remote control software interface has been developed implementing all the levels of interactions of users with the variables to be acquired/modified on the test-rig (PLC interface) through the virtual machine in POLITO servers. The working principle is based in the usage of a local PLC (compactRIO, fig.2.18) which receives the input/output analog signals from/to the test rig through Ni modules connected to MFCs (0-5 mV signals) and electronic load ( GPIB connection).

The PLC software will communicate by Ethernet protocols to a virtual machine, hosted in POLITO servers (where the control software will be installed), allowing the users interaction. In addition there is a database (also hosted in POLITO servers) will store all the test-rig data in input/output (fig.2.19).

The control interface will be accessible by web anywhere in the world.



Figure 2.15: Manual control panel.

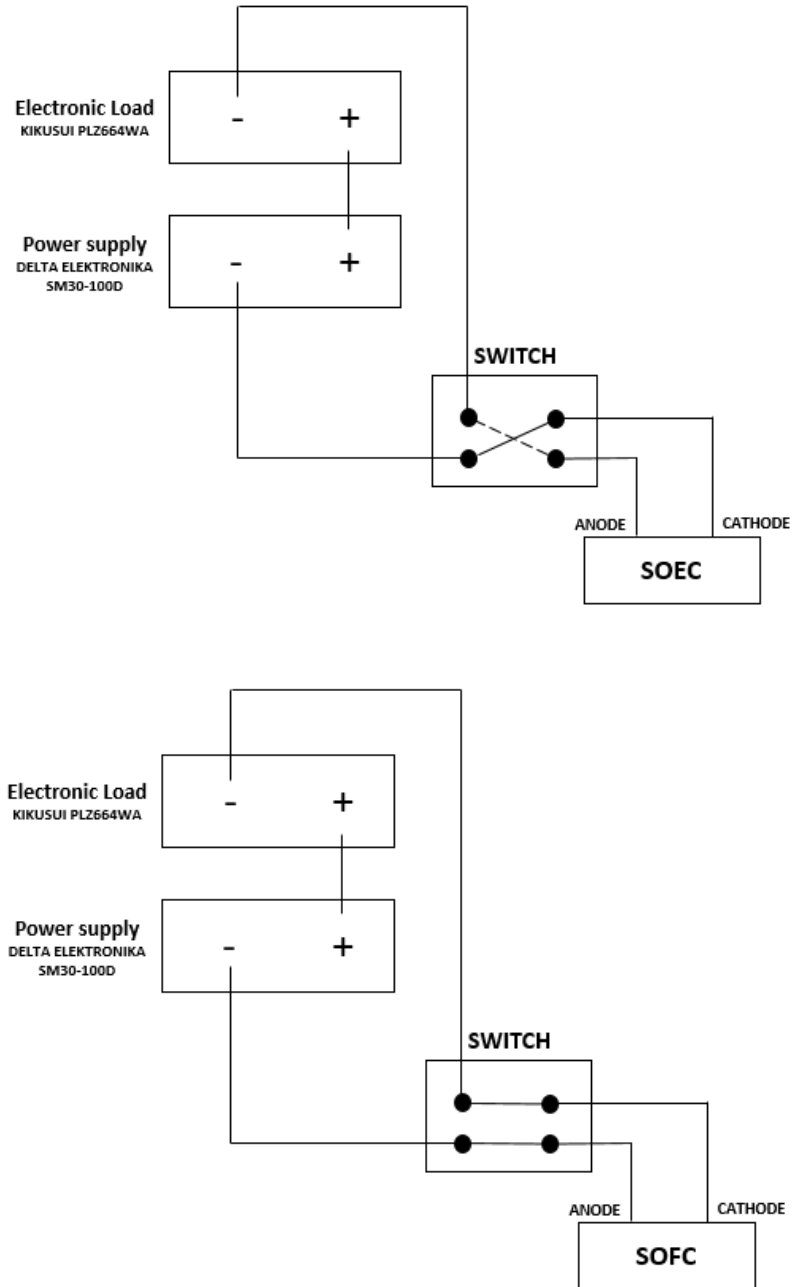


Figure 2.16: SOEC and SOFC electronic circuits



Figure 2.17: Manual control panel: PID



Figure 2.18: CompactRio

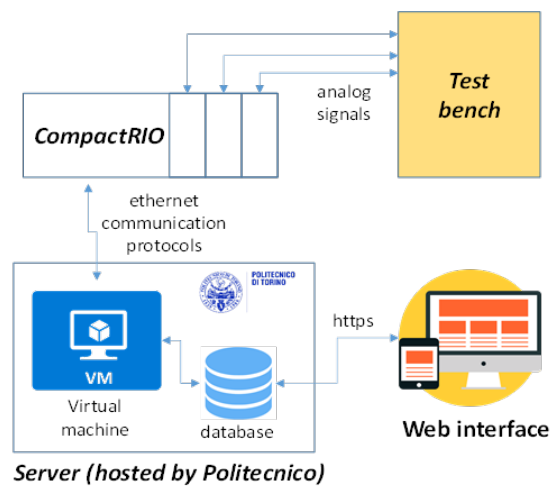


Figure 2.19: Remote control system scheme

# Chapter 3

## Labview Simulation and Teachy software

Laboratory Virtual Instrument Engineering Workbench (LabVIEW) is a system-design platform and development environment for a visual programming language from National Instruments. LabVIEW is commonly used for data acquisition, instrument control, and industrial automation on a variety of operating systems (OSs) [22]. The main target of this work is to test the LabVIEW software by implementing a simple system in which the physical measurements are acquired and the instrument deployed are controlled.

### 3.1 LabVIEW (National instruments) Hardware

The system hardware is composed by:

- *Compact DAQ*, which allows the synchronization and acquisition of data from analog input/output modules.
- *National AI/AO modules*, physical connected to the Compact DAQ, they enable the communication with the PC (through a USB cable) with input and output signals.
- *Mass flow meter* (Bronkhorst – El Flow Select), used to acquire mass flow rate measurement, it is connected to the National AI module, with a current input signal of 4-20 [mA] and powered through a transformer.
- *Mass Flow controller* (Bronkhorst –El Flow Select), used to acquire and control the mass flow, It is connected both to the National AI and AO modules, with current input/output signals of 4-20 [mA] and powered through a transformer.

- *Thermocouples B and K*, used to acquire high and low temperature measurements; with a temperature range around  $-200/1260\text{ }C^{\circ}$  for thermocouple K and  $50/1800\text{ }C^{\circ}$  for thermocouple B, they are connected to the National Analog Input module.

As shown in figure 3.1, the thermocouples and mass flow meters capture the temperature and mass flow measurements, the values of these physical quantities are sent to the input modules connected into cDAQ system through current signals with a range between 4 (minimum value) to 20 mA (maximum value). These signals are acquired and displayed to the PC through a USB cable.

The mass flow controller allows also the reverse communication, in this case through a command on the software interface it is possible to control the measuring instruments. This type of signal can be transmitted only via output module electrically connected to the cDAQ system.

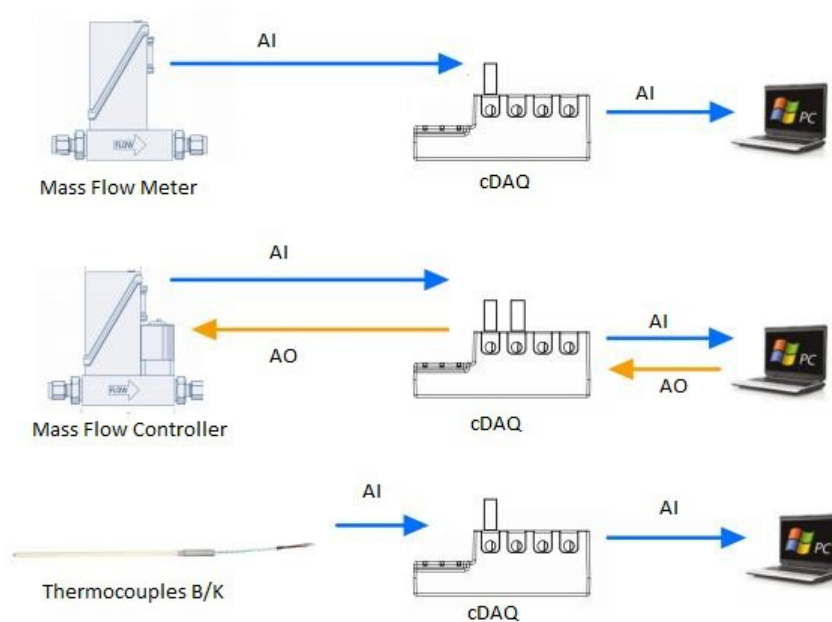


Figure 3.1: Labview cyber signals

The electrical connections between the mass flow meter and controller, the power supply and the National AI/AO modules are shown in more detail in the figure 3.2,3.3

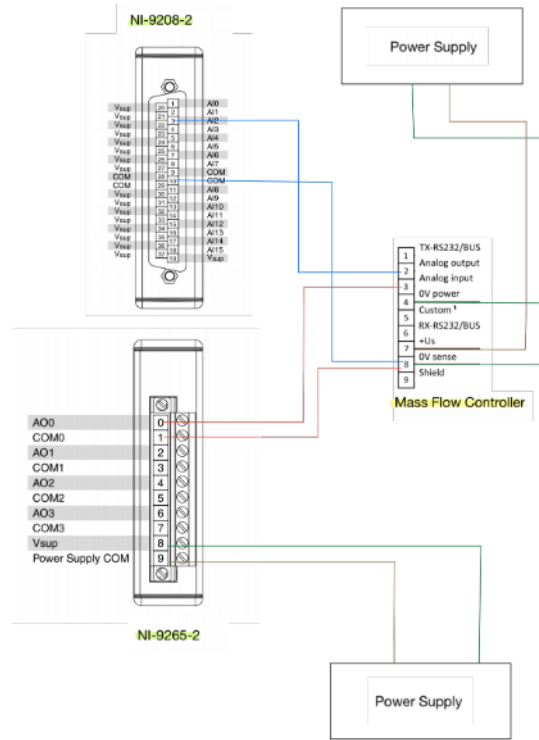


Figure 3.2: Mass flow controller electrical connection

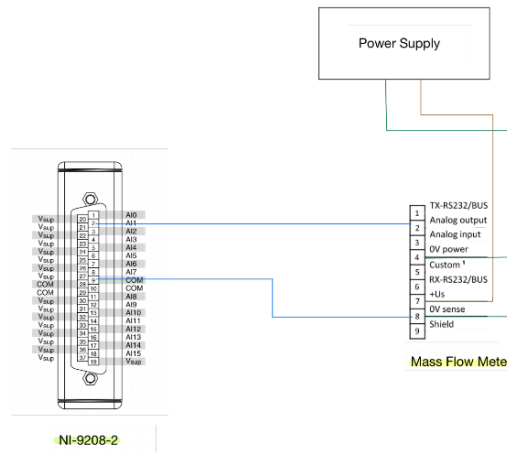


Figure 3.3: Mass flow meter electrical connection

## 3.2 LabVIEW (National instruments) Software

LabVIEW (National Instruments) is a development environment based on a visual programming language. The LabVIEW programs imitate the physical instruments present in any laboratory for this reason are called virtual instruments, or VIs. Every VI uses functions that manipulate input from the user interface and display that information or move it to other files or other computers [23]. LabVIEW programming environment contains the following three components:

- *Front Panel*, represents the user interface, containing controls and indicators terminals.
- *Block Diagram*, determines the functionality of the virtual instruments through graphical source codes.
- *Icon and connector pane*, give the possibility to generate subsystems.

### 3.2.1 Front Panel

The front panel is the user interface of the VI. It is based on controls and indicators, which are the interactive input and output terminals of the VI, respectively [23]. *Controls* simulate instrument input mechanisms (like line knobs, push buttons) and supply data to the block diagram of the virtual instruments [23]. *Indicators* simulate instrument output mechanisms and display output data (with graphs, LEDs) acquired from the block diagram [23]. By looking the figure 3.4 which displays the control/indicator functions used in the case study, it is possible to point out:

- **Numeric and slide indicators**, that allow to visualize mass flow, ambient and oven temperature values.
- **Numeric and slide controls**, that allow to manage a mass flow controller and the experiment duration.
- **Boolean indicators**, in particular two Boolean warning light related to temperature and mass flow rate. This tool enable to monitor both these physical measurement by providing an alarm signal when they exceed a certain level.
- **Waveform charts**, showing the temperature and mass flow rate evolution in time at a constant rate.

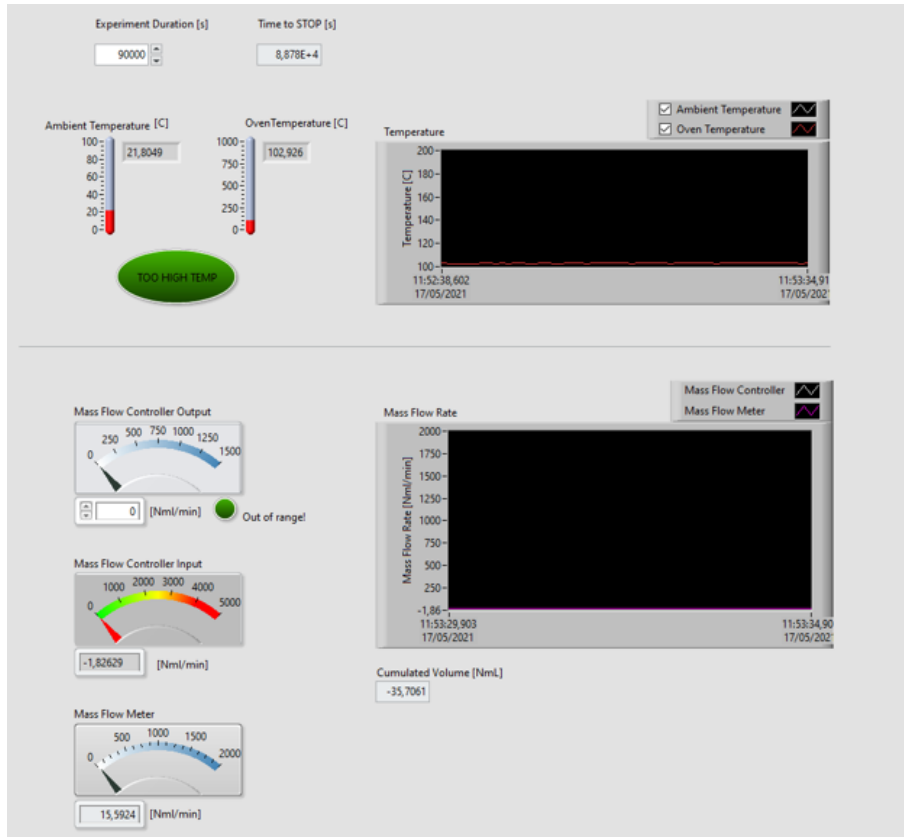


Figure 3.4: Case study: Front Panel.

### 3.2.2 Block diagram

To control the front panel objects, graphical codes representing all the functions are required.

The block diagram contains this graphical source code in which the objects are based on *terminals* and *nodes* connected with *wires* [23].

**Terminals** are entry and exit ports that exchange information between the front panel and block diagram [23]. Terminal types include: control, indicator and node terminals. The control and indicator terminals available on the block diagram correspond to those present in the front panel. During execution, the data inserted in the front panel reaches the block diagram via control terminals, then, passes through the nodes functions and arrives at the indicator terminals, where exiting from the block diagram will appear in front panel indicators.

In the figure 3.5, example of terminals are:

- **DBL**, depending on the direction of the data flow, it can be control or indicator type. In figure 3.5 there are six indicator terminals, used to display in front panel the values of *ambient and oven temperature, mass flow meter and controller, the cumulated volume and the experiment duration* and two control terminals, in order to set up the *mass flow controller output and the experiment duration*.
- **Constants**, used to supply fixed data values to the block diagram, useful to create computational blocks and to define limit values (in temperature and mass flow rate).

For what concern the **Nodes**, they are objects on the block diagram that have inputs and/or outputs and perform operations when a VI runs [23].

Nodes types include: functions, subVIs and structures. In the figure 3.5, example of Nodes are:

- **Daq Assistant**, belonging to the function type category, it is used to acquire signals coming from mass flow controller, mass flow meter and thermocouples.
- **Mathematical functions**, within this group are present all the computational functions used for mathematical operations.  
*Addition, division and multiplication functions* are deployed to convert the signal from [A] to [Nml/min] and viceversa.  
*Greater or less functions* are used to create a limitation in temperature and mass flow values.  
*Integration function block* are deployed to integrate in time the mass flow rate, in the way to compute the cumulated volume.
- **While loop**, belonging to the structure type category, is used to execute the system until the end of the experiment time.
- **Write to file**, is a node function used in order to write and store data into a Microsoft Excel file (.xlsx).

To transfer data among block diagram objects, the **Wires** are needed. In the figure 3.5, wires connect the control and indicator terminals to the different nodes of the system. Each wire could be different in terms of colors and thicknesses, depending on data types.

### 3.2.3 Icon and connector pane

An **icon** is a graphical representation of a VI, could be an images or a text. In the figure 3.5, icons are used to represent subsystem containing mathematical operations.

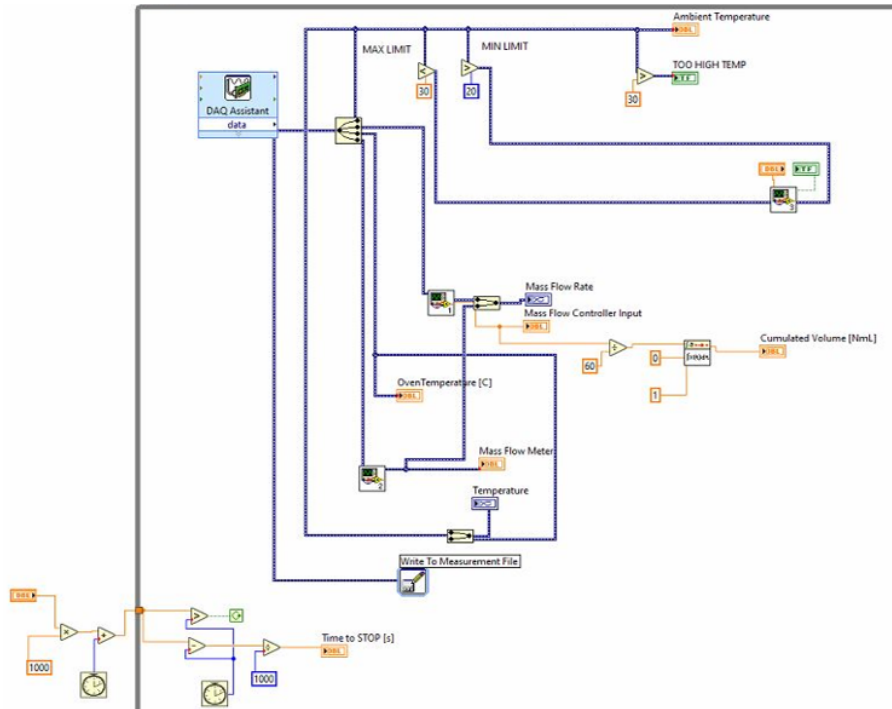


Figure 3.5: Case study: Block diagram.

To use a VI as a subVI, a **connector pane** is necessary. The connector pane is a set of terminals related to the controls and indicators of that virtual instrument, it defines the inputs and outputs that can be wired to the virtual instrument. [23].

### 3.3 Case study

#### 3.3.1 Acquisition - DAQ Assistant

Starting from the hardware explained in the section before, the first step of the Labview software analysis is to create a communication between the physical instruments (Hardware) and the software itself. To do that, the DAQ Assistant Block need to be inserted in the Block Diagram in the way to acquire data from mass flow controller, mass flow meter and thermocouples. The DAQ Assistant Block (figure 3.6) can be found by selecting “Input” in the Functions popup.

For a proper operation the type of input signal and the physical channel for the communication need to be specified in the DAQ Assistant Block characterization. For the the temperature measurements, the thermocouple specifications is inserted and 'Thermocouple setup' is selected (figure 3.7), which gives a signal in  $[C^{\circ}]$ .

In the case of mass flow rates measurements, the 'current input setup' has to be



Figure 3.6: DAQ Assistant block

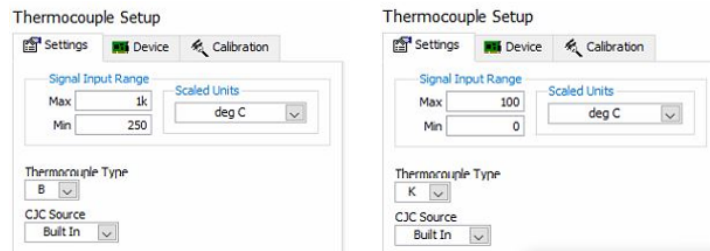


Figure 3.7: Thermocouples B and K setup

selected (figure 3.8), which returns a signal in [A] (ranging between 0,004-0,02 A).

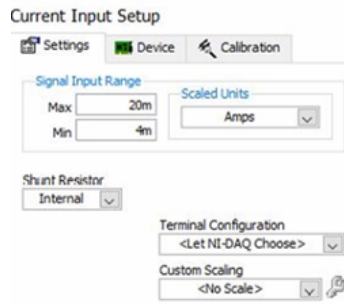


Figure 3.8: Current input setup

### 3.3.2 Data analysis

Once acquired the data are *conditioned, plotted and stored*.

The *conditioning* of data in the Block Diagram can be done by converting the input current signals (AI) [A] coming from the DAQ Assistant into [Nml/min]. This can be done through mathematical operators and numeric constants. In the figure 3.9 the *Main(SubVI).vi* blocks contain the conversion operations.

The *plotting* of the evolution of signals in time can be done through Waveform Charts and graphs, while the instantaneous values can be visualized through proper

numeric and slide controls and indicators of temperature and mass flow rate, visible in the Front Panel. In the figure 3.9 the orange blocks represents indicators terminals and the blue blocks represent the Waveform Charts, one for the temperature and one for mass flow rates. Finally, in order to write and *store* data into a Microsoft Excel file (.xlsx), the 'Write to Measurement File' block is inserted in the Block Diagram.

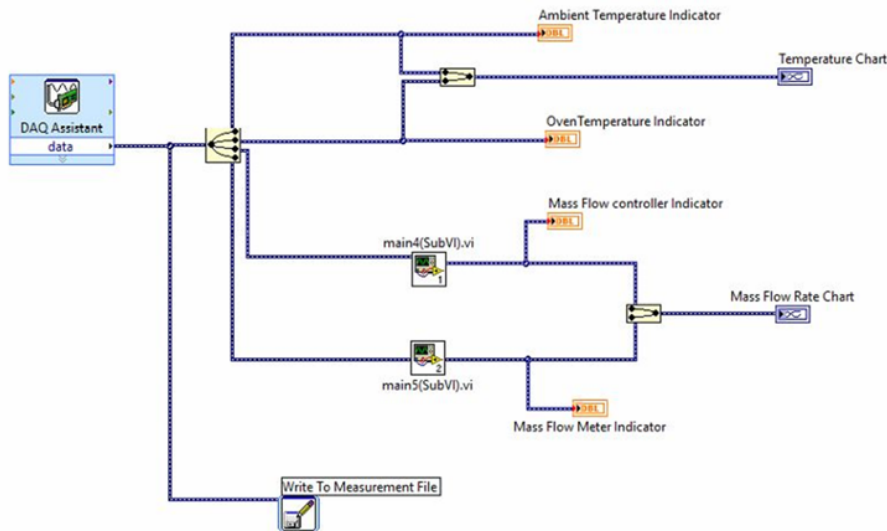


Figure 3.9: Schematic block diagram with subsystems

For what concern the front panel in figure 3.10 the indicators are positioned on the left side. They give the instantaneous values of Temperature and Mass flow Rates. Instead the WaveForm Charts are positioned on the right side, plotting Temperature / Mass flow Rates versus time.

### 3.3.3 Control output

The possibility to manage the physical devices can be provided through control signals (AO) coming from the LabWiev software. To handle the Mass Flow Controller a second DAQ Assistant Block is used.

Even in this case the type of output signal and the physical channel need to be specified in the DAQ Assistant Block. The characterization of the signal takes place in the 'current output setup' (figure 3.11), in which is specified the current range in [A] (between 0,004 and 0,02 A). The signal must be properly converted in [A] before going to the DAQ Assistant, for this purpose a Numeric Control Block is inserted and connected with the inlet of the DAQ Assistant Block. At this point he user can select the desired Mass Flow Rate in [Nml/min] through the Front Panel (3.12).

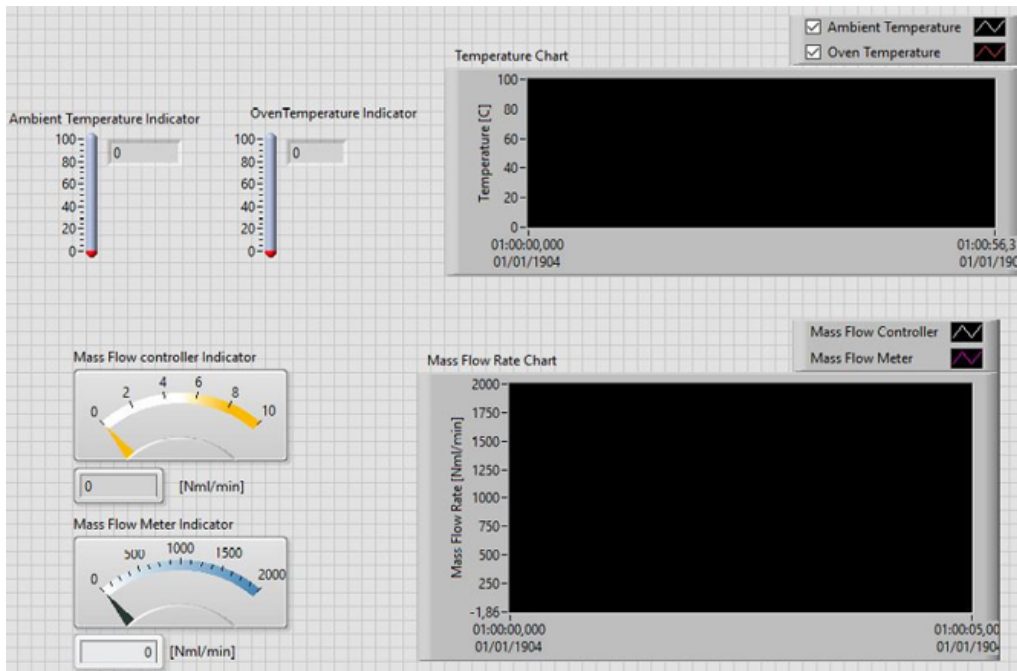


Figure 3.10: Front panel user interface

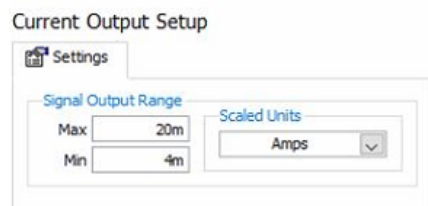


Figure 3.11: Current Output Setup

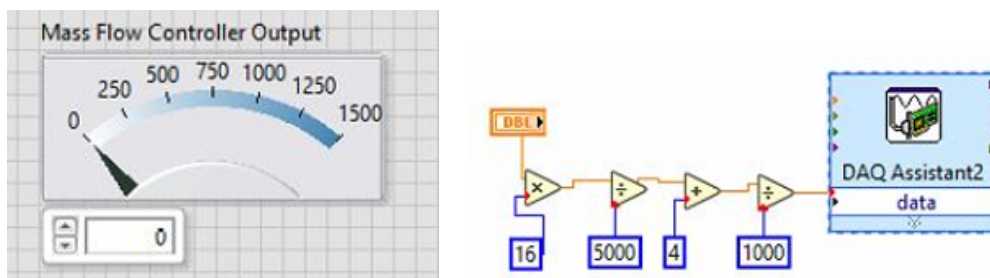


Figure 3.12: Mass flow rate selection and consequentially block diagram.

### 3.3.4 While loop

A While Loop, which executes the system until a certain condition occurs, has been inserted. In the case study, the condition to exit the loop is the end of the experiment time inserted by the user which is translated in a specific Boolean value. A numeric indicator is placed in the front panel to show the residual time (3.13). The time imposed by the user is used to check the loop-exit-condition and to compute the residual time.

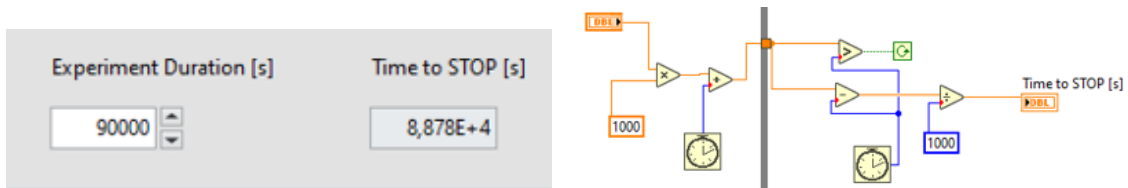


Figure 3.13: Experiment time duration and consequentially block diagram.

### 3.3.5 Further implementation

Further tools are deployed in the LabView Software. In particular an indicator which provides the information about the amount of gas passed in [NmL] through the MFC (from the beginning of the experiment) has been inserted in the Front Panel. The value is computed by integrating in time the mass flow rate of gas, through an Integration Block, which gives the cumulated volume (figure 3.14).

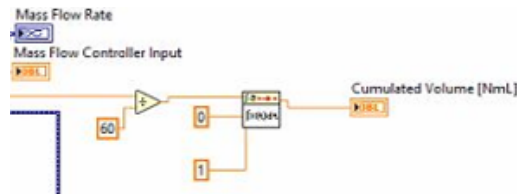


Figure 3.14: Cumulated volume block diagram.

In addition an alarm-indicator has been inserted in the Front Panel, warning the user when too high Temperature is reached. A second alarm-indicator has been inserted, warning the user when the inserted mass flow rate (AO) exceed an upper limit (figure 3.15).

Besides the alarm indicators, some controls have been integrated to the command (AO signal) of the MFC:

- When the temperature of thermocouple B is outside of a predefined range, the mass flow rate is stopped, in the way to arrest the operation.

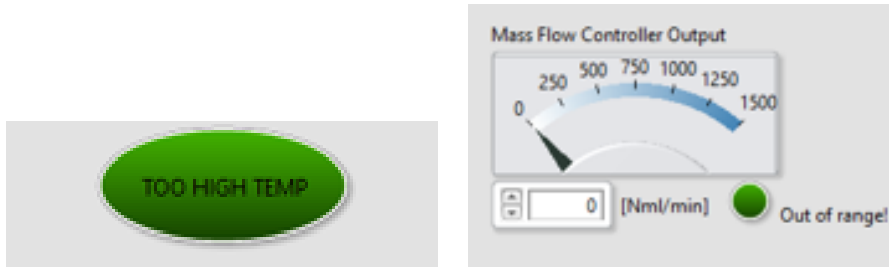


Figure 3.15: Alarm indicators related to temperature (right side) and mass flow rate (left side).

- When the the output signal given by the user exceeds the upper limit, the mass flow is imposed equal to the upper limit itself, which is a prefixed value.

A possible deployment of the system explained in this chapter was to integrate it into the test bench, in order to control the experimental work through the LabWiev software.

In the figure 3.16 is showed the Compact DAQ with the National AI/AO modules physical connected during the operation.



Figure 3.16: Compact DAQ during the operation.

# Chapter 4

## Teachy Software

Teachy is a software for the remote control of a test bench of the Department of Energy Polytechnic of Turin. The objectives of the experimental work on this software was to provide, through a careful analysis of the various sections, improvements to the Teachy project.

In particular, a first phase of the work was to find various malfunctions within the software during the operation, and in the second phase we tried to make the system easier to use.

The software can be freely used by students on and off-site for study and experimentation. The system was developed using a micro service architecture distributed on two physical servers. Each micro service takes care of functions related to its domain.

In this software there are 3 types of users with different privileges in the system:

- *Root*, created directly on the Database, will have the ability to manage Administrator accounts.
- *Administrator*, has access to all system functions and can create, view and delete *User* accounts.
- *User*, will only be able to log in if it is associated with a group active, is able to visualize the variables of the group to which it has been assigned and the logs for those variables.

The application is a web platform accessible from any browser and can be reached at the following address: <https://teachy-www.polito.it:8085/PoliTo>. In order to access the application features, the operator must log-in using the own credentials, username and password (4.2).

After logging in, the operator will be access to the platform. The dashboard shows a menu on the right and the contents of the sections on the rest of the screen. In the following paragraphs all the sections of the software program will be analyzed, in order to provide a greater understanding of the Teachy project.

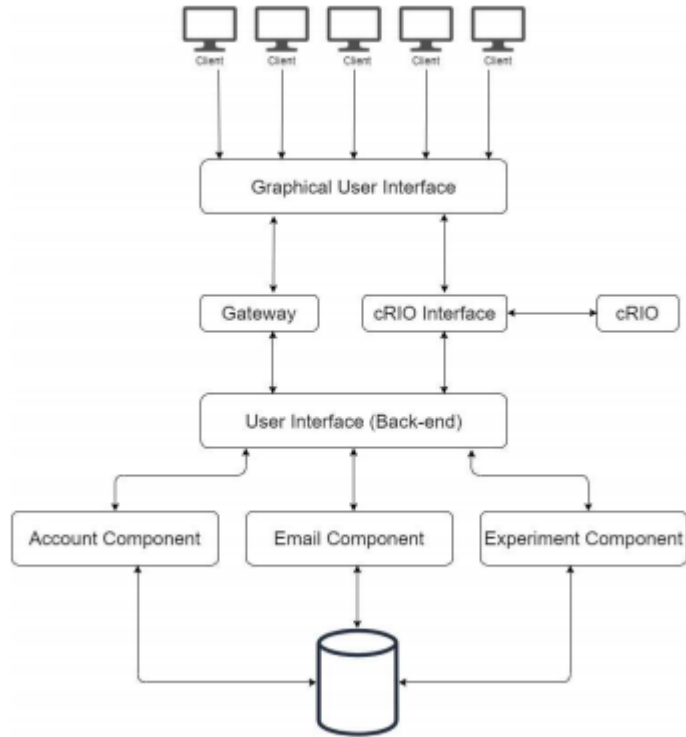


Figure 4.1: Teachy Architecture.

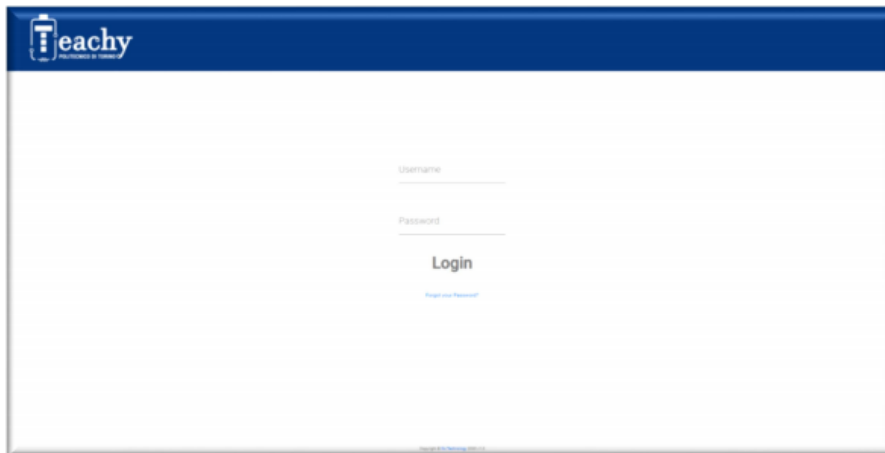


Figure 4.2: Teachy Login.

## 4.1 Dashboard

The menu contains different items based on the type of user logged in and on the status of the cRIO (compact RIO) associated with the system, whether under maintenance or not. Brief descriptions of the various program's items are listed in the following paragraphs to offer a software overview.

### 4.1.1 Menu account Root

The menu of the Root account (figure 4.3) has the items:

- *Home*, where the alerts related to the missing emails of activation are displayed.
- *Admins Management*, containing two subsections:
  - *Admins list* for the Administrators list registered on the system.
  - *Create admin* to create new Administrators.
- *Logout*, to log out from the platform.



Figure 4.3: Menu account Root.

### 4.1.2 Menu account Administrator

For what concern the Menu account Administrator (figure 4.4, there are the following items:

- *Home*, where the alerts related to the missing emails of activation are displayed.

- *Users Management*, containing two subsections:
  - *Users list*, for the Users list registered on the system.
  - *Create users*, where is possible to create new Users.
- *Variable Management*, containing two subsections:
  - *Variable list*, for the all variable list registered on the system.
  - *Create Variable*, where is possible to to create new variables, it is visible only when the system is under maintenance.
- *Groups Management*, containing three subsections:
  - *Group list*, a table showing all the working groups created.
  - *Create Group*, where is possible to create new groups.
  - *Assign Users*, through which users can be assigned to the created work groups.
- *Experiment Profiles*, containing two subsections:
  - *Experiment Profiles list*, a table showing all the Experiment Profiles created.
  - *Create Experiment Profiles*, where is possible to create new Experiment Profiles.
- *Script*, allows to send script files to cRIO and in addition it gives the possibility to start or stop the operation.
- *Experiment section*, allows monitoring the values of variables coming from the bench in real time. In addition in this section is possible to send set point values, check the status of the script (if it is execution or stop), the status of the logs, if there were alarms on the test bench.
- *Logs configuration*, allows to configure normal logs and quick logs for existing variable groups.
- *Command*, provides four commands for the operator:
  - *Safe* to secure the test bench and set the variable values to zero
  - *Enable Maintenance Mode / Disable Maintenance Mode* to enable or disable the maintenance mode.
  - *cRIO Configuration*, to configure the variables currently present on the bench.

- *Error Acknowledge*, to send an acknowledge for resolved alarms on the bench.
- *Logs*, allows to see the values saved in the Database represented on a graph on a temporal range, data can be exported to files .csv e .xlsx.
- *Delete Logs*, allows to eliminate logs located in the Database.



Figure 4.4: Menu account Administrator.

### 4.1.3 Menu account User

For what concern the Menu account User (figure 4.5, there are the following items:

- *Experiment section*, where the user can see the variable's values in real time and if allowed is able to change set up values.
- *Logs*, allows to see the values saved in the Database represented on a graph on a temporal range, data can be exported to files .csv e .xlsx.

## 4.2 Teachy items Description

In this paragraph, the various program's items listed in the previous section will be described in more detail.

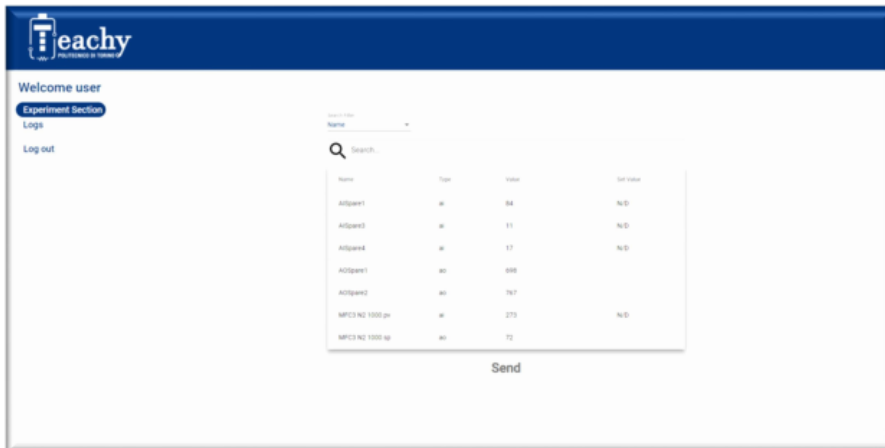


Figure 4.5: Menu account User.

### 4.2.1 Home

In the Home section it is possible to see a table with all the missing emails that have not been received due to several reasons like invalid address, full mailbox, etc. If there are no alerts the message 'no alert found' will appear.

### 4.2.2 Account Management

In these sections it is possible to create, view or delete accounts from the system except for Root type account.

#### 4.2.2.1 Admins List / Users List

In these sections it will be possible to view tables showing all the accounts present in the platform.

Entering with Root-type account it is possible to see the Admin list, or the User list in the case of Administrator-type account (figure 4.6). For each account listed in the table there is a field, which is "Active" if the user has completed the registration procedure.

To delete an account it is necessary to click on the "Delete" button and confirm the choice.



Figure 4.6: Admin list (right side) and User list (left side).

### 4.2.3 Account Creation

The accounts, as mentioned before, come from the appropriate section in the Roots and Administrators account menus for the creation of Administrators and Users respectively. Root accounts can only be created through direct action on the Database.

#### 4.2.3.1 Creation Admin/user

In the "Create User" and "Create Admin" sections it is possible to create accounts. To be able to realize an account, is necessary to fill in the form shown in figure 4.7, indicating the Email, the Registry Number, University, first name and last name. Once completed, the system will send an email to the address of mail specified to complete the account registration.

Figure 4.7: Admin Account Creation.

## 4.2.4 Variables Management

In these sections it is possible to manage the variables registered on the system. The variables can be visualized, modified, deleted, and created.

### 4.2.4.1 Variable list

In the "Variable list" section it is possible to view all the variables registered in the system.

To delete, create or change a variable in this section the system must be in maintenance mode (figure 4.8). Once you have made the necessary changes to the variables, to make them effective on the experiment bench, the information about the variables upgrading must be send to cRIO.

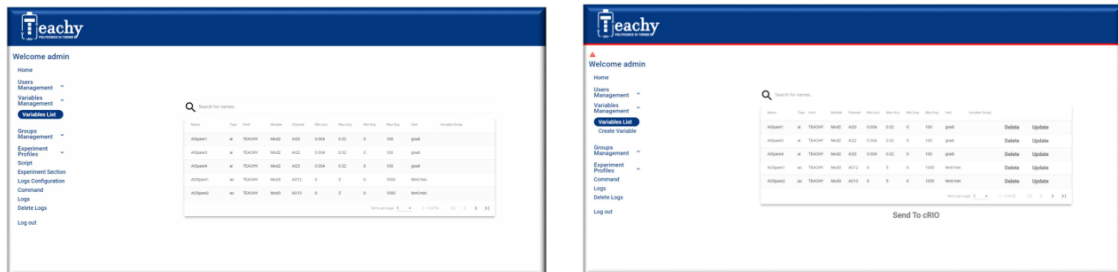


Figure 4.8: Variable list (right side) and Variable list in maintenance mode (left side).

### 4.2.4.2 Create variable

To create a new variable, the system must be in maintenance mode as mentioned before. Once under maintenance, the item "Create Variable" will appear with the form to be filled in (figure4.10.)

The "Variable Group" field is used for assigning fast logs.

## 4.2.5 Groups Management

Through the application it is possible to create temporary work groups where there are different User accounts.

Within the group the user could be assigned in two different roles:

- The *Head* role, there can only be one for each group, gives the possibility to the User to view and modify the variables assigned to the group.

The screenshot shows the 'Create a new Variable' form in the Teachy admin interface. The form is titled 'Create a new Variable' and contains the following fields:

- Variable Name:
- Type:
- Host:
- Module:
- Channel:
- Min Acq:
- Max Acq:
- Min Eng:
- Max Eng:
- Unit:
- Variable Group:

A 'Create' button is located at the bottom center of the form.

Figure 4.9: New variable creation

This screenshot is identical to Figure 4.9, showing the 'Create a new Variable' form in the Teachy admin interface. The form includes fields for Variable Name, Type, Host, Module, Channel, Min Acq, Max Acq, Min Eng, Max Eng, and Unit, with a 'Create' button at the bottom.

Figure 4.10: New variable creation

- The *Read-Only* role represents the Users who can only view the trend of the experiment. They can be more than one.

#### 4.2.5.1 Groups list

Trough the "Groups List" section it is possible to view the list of all existing groups (figure 4.11).

The section shows a tabular representation of the groups in which the group name , the start date and start time, the end date and time, and the experiment configuration associated with that group are represented. In this section it is also possible

to delete, through the “Delete” button, or modify, through the ”Update” button, a group.

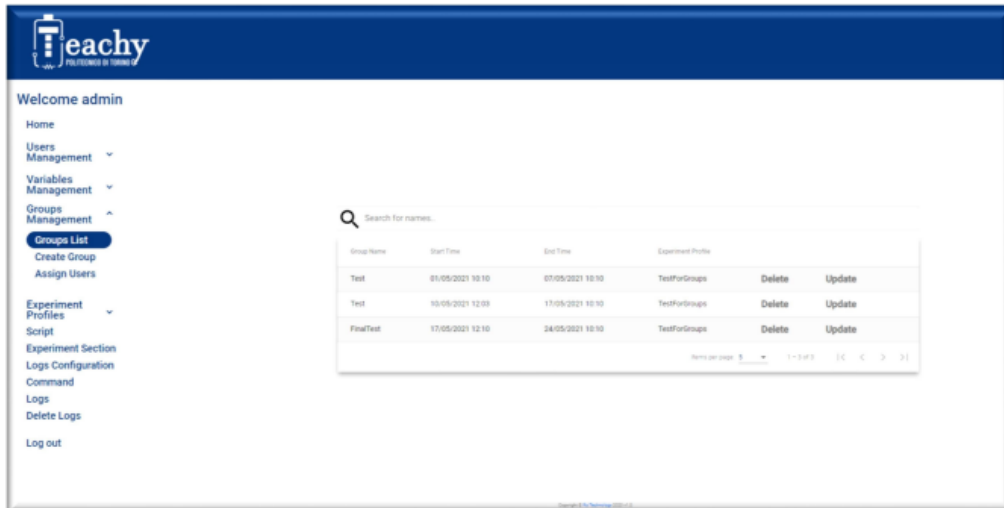


Figure 4.11: Group list.

#### 4.2.5.2 Create group

Through the ”Create Group” section it is possible to create a new group (figure 4.12).

Inside there will be a form that make the operator enable to set the name of the group, the experiment profile, the date and time of beginning and end of the group. Important to mention that is not possible to create overlapped groups in time within an existing one.

#### 4.2.5.3 Assign User

After creating a group it will be possible to assign the Users who will take part in the experiment through the “Assign Users” section (figure 4.13).

Inside there is a table showing the information of the group together with the item ”Assigned Users ”, representing the Users who are assigned to the group. If the group does not have Users assigned the field will appear empty.

To start the assignment procedure, the operator should select the group to which he wants to assign the Users. By clicking, a pop-up opens with 2 tables showing all the Users registered in the system (figure 4.14). At this point it is possible to choose the User-type (Head or Read-Only User).

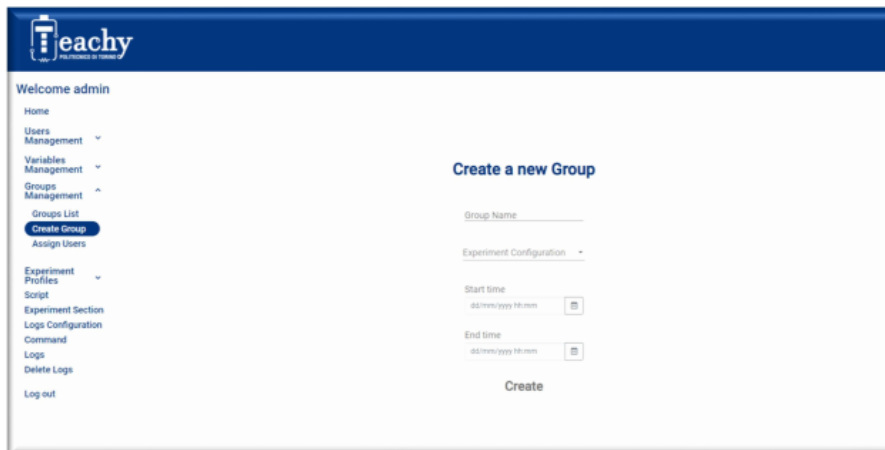


Figure 4.12: Group creation.

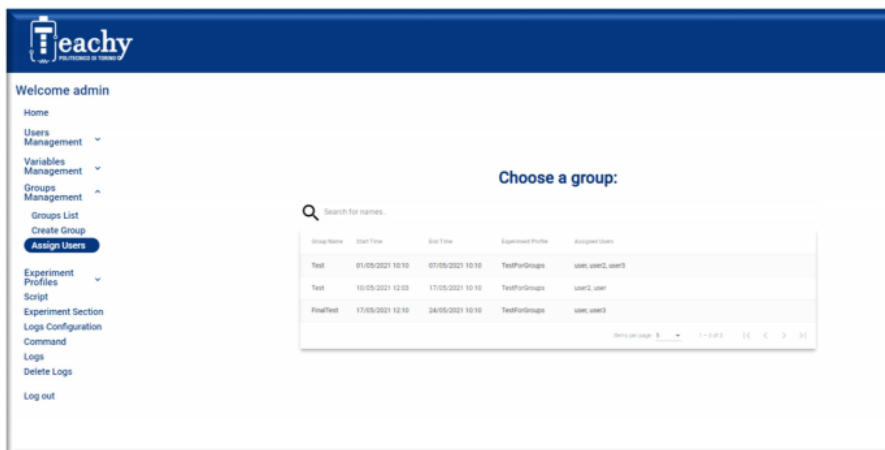


Figure 4.13: Assign User list.

## 4.2.6 Experiment profile

Within the application it is possible to create subsets of variables to be assigned to work groups.

### 4.2.6.1 Experiment list

Through *Experiment profile List* it is possible to view all the Configurations present in the system. They are represented in a tabular way in which the name of the Configuration and the names of the chosen variables are reported (figure 4.15). In addition it's possible delete, through the "Delete" button, or modify, through the

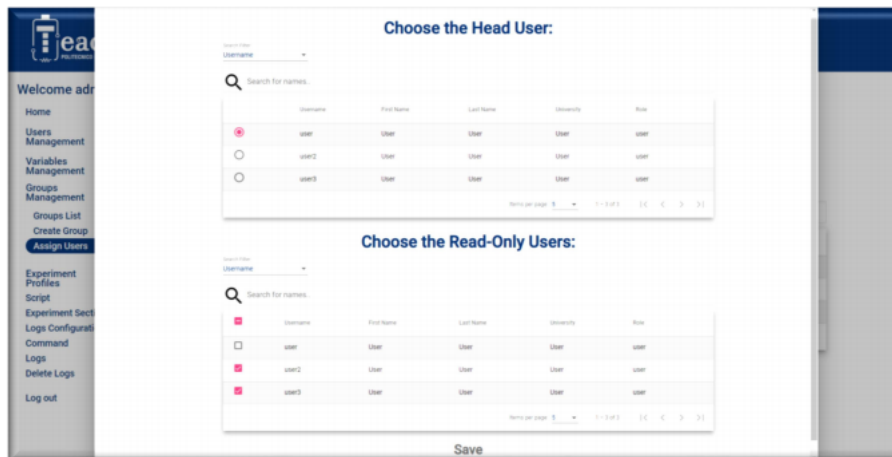


Figure 4.14: Assign User type.

“Update” button, a configuration.

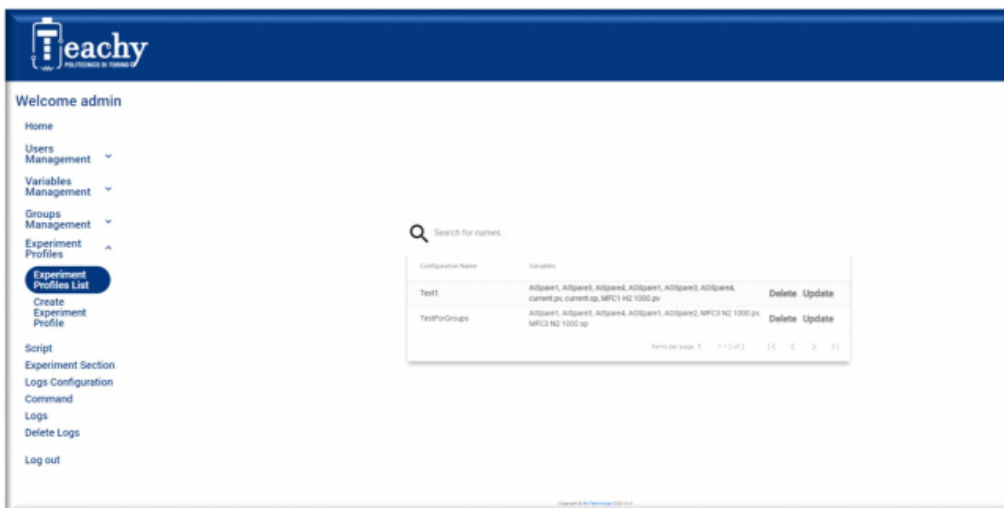


Figure 4.15: Experiment profile List.

#### 4.2.6.2 Create Experiment profile

It is possible to create a new Configuration through the *Create Experiment Profile* section (figure 4.16).

In order to do that the name and the variables to be included in the configuration must be specified.

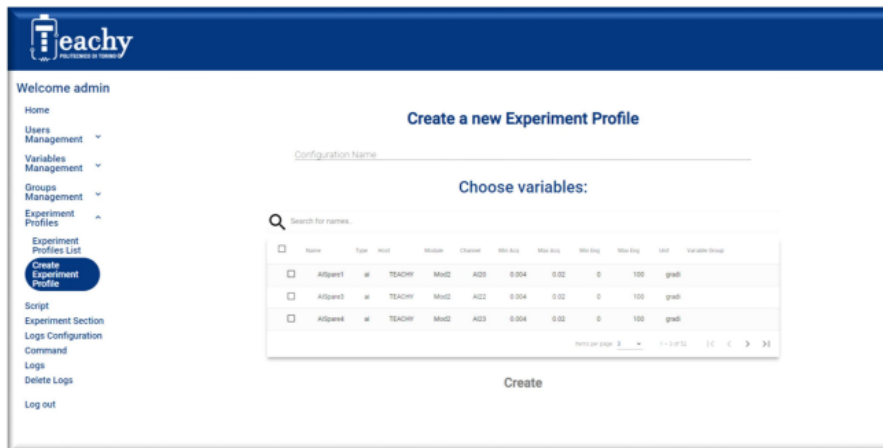


Figure 4.16: Create Experiment profile.

## 4.2.7 Script

Through the *Script* section it is possible to load, start or stop a script on the cRIO. The section shows an input field in which you can choose the file to upload in .json. created in a second software (figure 4.17). Once the file has been chosen, by clicking on the *Upload* button the file is sent to the desk. If the upload is successful, a pop-up will appear with the confirmation of the upload, in case otherwise the error will be reported in the pop-up. Once uploaded successfully, the section will show the file name and its status (figure 4.18):

- *file-name currently uploaded*, when the file is uploaded but has not been started.
- *file-name currently running*, when the script is running.
- *Kill file-name*, to stop a running script.

## 4.2.8 Experiment section

The *Current Experiment* section allows real-time monitoring of the status and data coming from the test bench. In function of the typology of account the screen changes.

### 4.2.8.1 Experiment section Administrator

In this section, *Administrators* can monitor in real time the values of the variables of the whole system and change the *Set Points* values through the table on the left

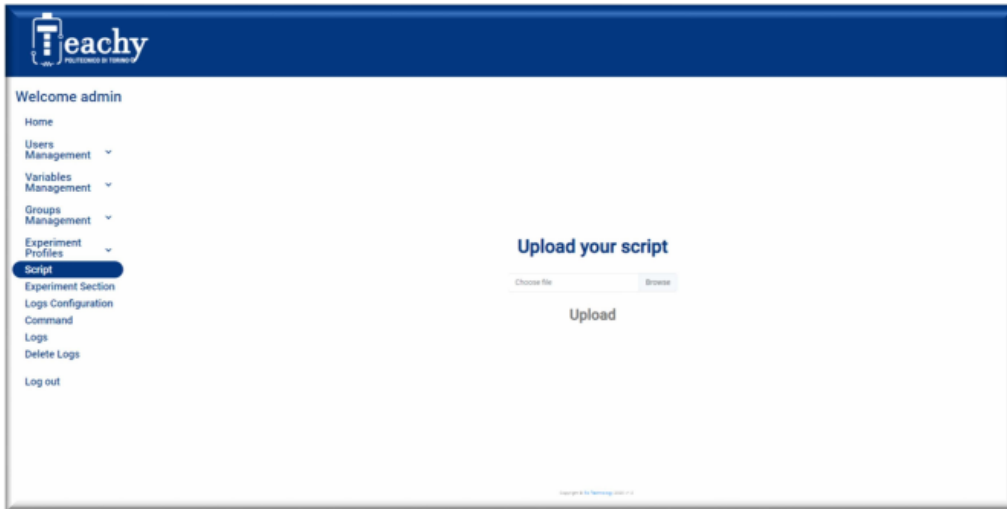


Figure 4.17: Script section.



Figure 4.18: Condition to run the script (right side) and condition to stop the script (left side).

of the figure. The table shows the name of the variables, the value updated in real time by the test bench, and the *Set column Value* where there will be the desired values that the *Administrator* decides to insert. If the value is above above or below the threshold of that variable the system will warn the operator. Once the desired *Set Points* have been inserted but don't sent, the system will notify the operator with a red writing next to the Send button with the wording Variables not sent. The box on the top right of the figure 4.19 is used for system status monitoring, is reported:

- The status of the normal logs in the Database (true or false)
- The status of the quick logs in the Database (true or false).
- The status of the Script (if the Script is loaded, running or stopped)

- if the application is connected or not to cRIO (“Connected” or “Disconnected”).

The table at the bottom right of the figure 4.19 shows all the errors coming from the the test bench with the date and time and the content of the alarm. It is possible to delete the alarms through the *Delete* button.

When the system is in alarm it will not be possible to insert set points values.

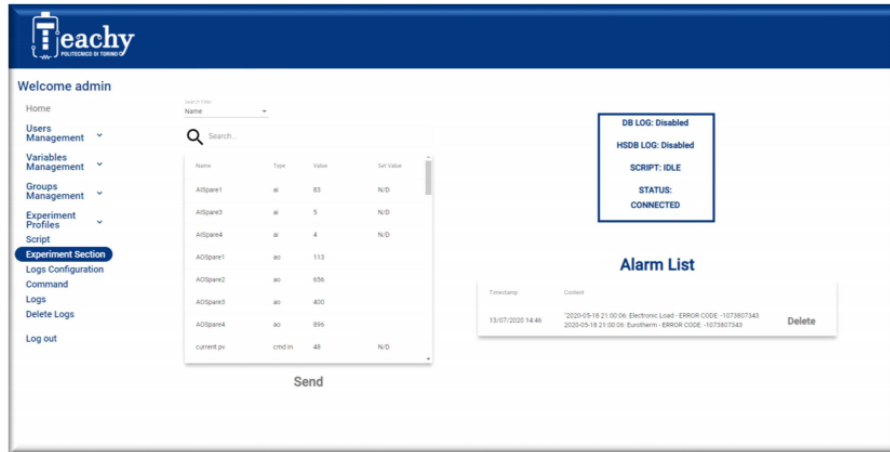


Figure 4.19: Experiment section Administrator.

#### 4.2.8.2 Experiment section User

In this section, the Users can see only the table showing the real-time data for the variables associated with the group to which it belongs (figure 4.20).

The Head User will be able to modify the Set Points of the variables assigned while Read-Only Users can only visualize the data. By clicking on the corresponding line, it is possible to insert a set up value. In the same way of the section before, if the value is above or below the threshold of that variable the system will warn the user. When a Head User submits a Set Point value, all Read-Only Users online will be notified regarding the changes he made. Instead, when the system is in alarm, the Users will be notified and the submission of the Set Point value will be blocked.

#### 4.2.9 Logs configuration

The software gives the possibility to enable fast saving (more frequently) of variables' groups through high speed logs. To enable this logs it is necessary to go to *Logs Configuration* section and choose, through a calendar, the date and time of logs activation. The two inputs on the right of the figure 4.21 are used to configure the

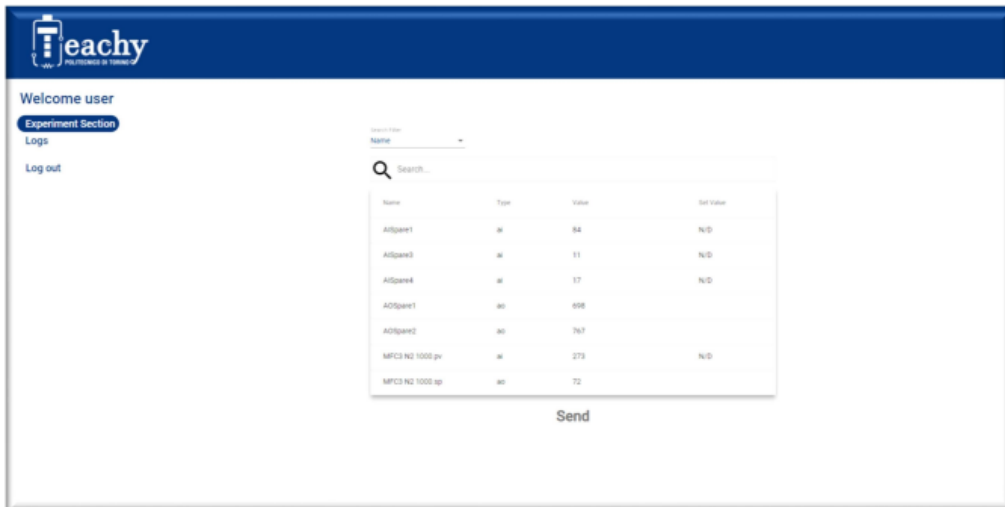


Figure 4.20: Experiment section User.

quick logs of variables' groups. The first, allows the operator to choose the date and time. The second one instead requires the variables' groups name. In addition, in the lower part of the figure 4.21, any fast logs currently active and the their expiration date are shown.

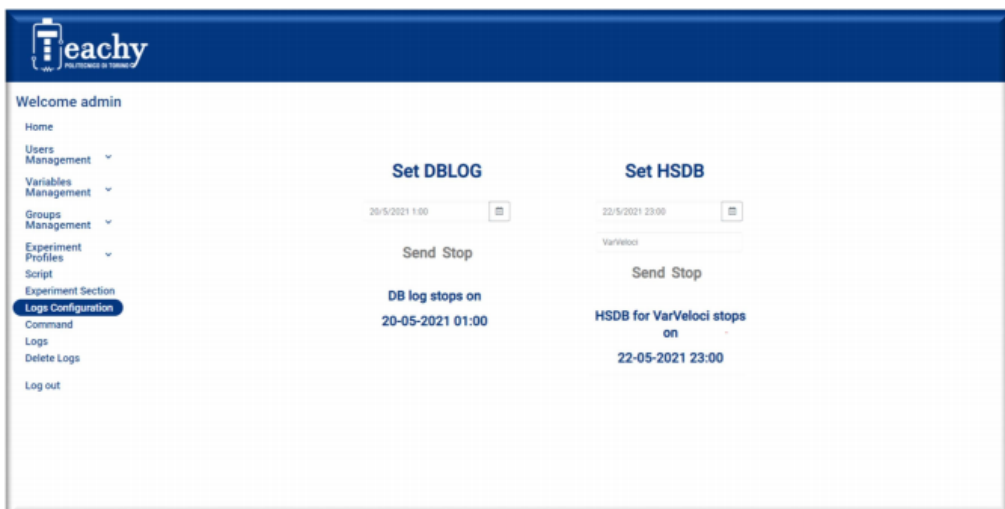


Figure 4.21: Logs configuration.

### 4.2.10 Command

In the command section there are some commands useful for interacting with cRIO (figure 4.22).

The *Safe* button puts the system in safety and sets the value of all variables to zero. The *Enable Maintenance Mode* and *Disable Maintenance Mode* buttons are used respectively for enable and disable maintenance mode.

The *cRIO Configuration* button asks cRIO to configure the variables and overwrites in the application. When the system is in alarm, the *Acknowledge* button appears to send the Acknowledge command of the alarms resolved with cRIO.



Figure 4.22: Command section.

### 4.2.11 Log

Within the *Logs* section, it is possible to visualize the historical data of the selected variables. In order to proceed with the search, a variable or more must be chosen from the drop-down menu (figure 4.23). Once the variable has been chosen, the desired time range must be selected, this is possible through the two input fields *Start time* and *End time*.

The resulting data are displayed on a time chart (figure 4.24) and the result can be exported in format *.csv* and *.xlsx* files. With the *Reload Logs* button the graph is updated with the latest data received, while with the button *Change Variables* it is possible to change the previously search parameters.

It is possible to delete the logs via the *Delete Logs* section by indicating the time range that you want to cancel.

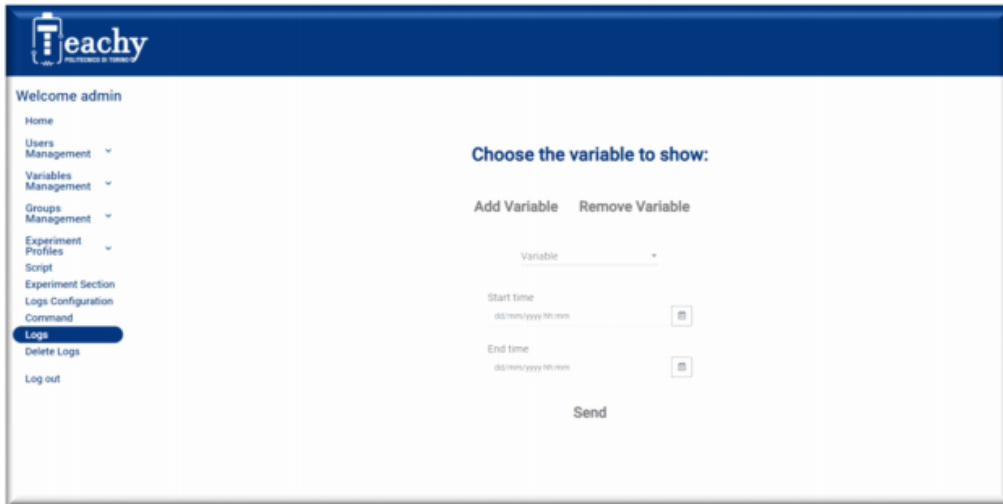


Figure 4.23: Log section.

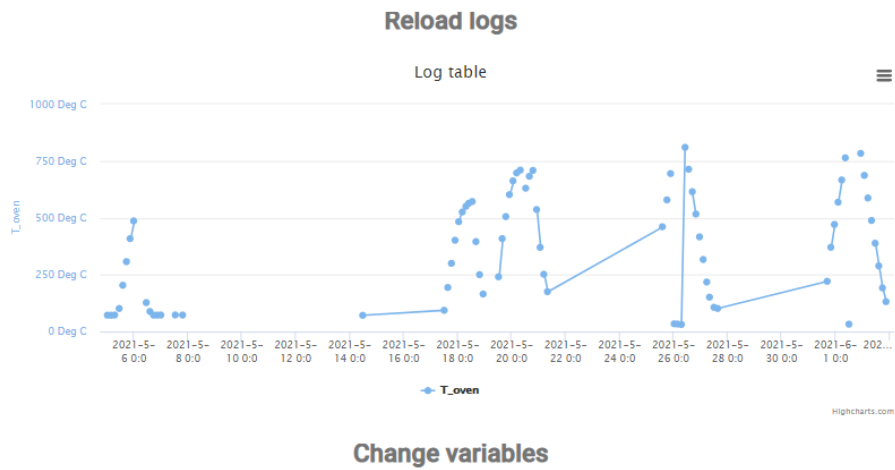


Figure 4.24: Log chart.

# Chapter 5

## SOEC test

The experimental work is composed by two main part. The first part is determined by calibration of those fundamental device for the correct functioning of the cell, such as the mass flow controllers of the test bench.

The second part is characterized by the assembly and the analysis of the cell which can be divided in four different successive step: test bench setting up procedure, start up, cell testing and switch off.

For all the steps listed there is a standard procedure that will be explained in the following paragraphs.

### 5.1 Mass flow controllers Calibration

The mass flow controllers calibration is carried out by comparing the flow measurements of the test bench (via PIDs) and a volumetric flow meter separated from the system. The procedure can be summarized in five points:

1. Manual insertion of set point values in [Nml/min] through PIDs installed in the test bench.
2. Values' reading via PID displays in [Nml/min].
3. Measurements verification through a volumetric flow meter separated from the bench (Definer 220, figure 5.1). With an accuracy of  $\pm 1\%$  percent of reading experiment [24] the working principle is based to positive displacement technology.
4. Calculation of set point errors in percentage, as the difference between the set point values inserted trough PIDs and and the values measured with the calibrator (Definer 220), divided with this last calibrator measurement.



Figure 5.1: Definer 220 [24]

5. Calculation of reading error in percentage, as the difference between the values displayed via PIDs and and the values measured with the calibrator (Definer 220), divided with this last calibrator measurement.

Table 5.1: MFC 1 calibration.

$H_2$				
Set point value [Nm <sup>3</sup> /min]	Measured value [Nm <sup>3</sup> /min]	Read value [Nm <sup>3</sup> /min]	Set point error [%]	Read error [%]
50	55.9	52.0	11.9	7.60
100	102.5	100.8	2.50	0.688
300	302.8	302	0.933	0.265

Table 5.2: MFC 2 calibration.

$H_2$				
Set point value [Nm-l/min]	Measured value [Nm-l/min]	Read value [Nm-l/min]	Set point error [%]	Read error [%]
50	55.5	50.0	11.0	11.0
100	102.5	100.0	2.50	2.50
300	296.7	301.0	-1.10	-1.43

Table 5.3: MFC 3 calibration.

$N_2$				
Set point value [Nm-l/min]	Measured value [Nm-l/min]	Read value [Nm-l/min]	Set point error [%]	Read error [%]
50	47.7	50.0	-4.60	4.60
100	99.1	101	-0.900	-1.88
300	299	301	-0.166	-0.498

Table 5.4: MFC 4 calibration.

$N_2$				
Set point value [Nm-l/min]	Measured value [Nm-l/min]	Read value [Nm-l/min]	Set point error [%]	Read error [%]
50	57.7	51.0	15.0	12.7
100	107	101	6.80	-5.74
300	300	301	-0.0667	-0.399

Table 5.5: MFC 6 calibration.

$N_2$				
Set point value [Nm-l/min]	Measured value [Nm-l/min]	Read value [Nm-l/min]	Set point error [%]	Read error [%]
50	56.5	50.0	13.0	13.0
100	108	100	8.40	8.40
300	308	300	2.56	2.56

Table 5.6: MFC 7 calibration.

$N_2$				
Set point value [Nm-l/min]	Measured value [Nm-l/min]	Read value [Nm-l/min]	Set point error [%]	Read error [%]
50	51.2	51.0	2.40	0.392
100	101	101	1.30	0.297
300	300	301	0.100	-0.233

Table 5.7: MFC 5 calibration.

Air				
Set point value [Nm-l/min]	Measured value [Nm-l/min]	Read value [Nm-l/min]	Set point error [%]	Read error [%]
200	210	202.4	5.10	3.85
280	292	282.4	4.29	3.39
400	413	404	3.38	2.55

Table 5.8: MFC 10 calibration.

CO				
Set point value [Nm <sup>3</sup> /min]	Measured value [ml/min]	Read value [Nm <sup>3</sup> /min]	Set point error [%]	Read error [%]
50	60.7	50.3	21.5	20.7
100	111	100	11.4	10.9
300	310	300	3.40	3.26

Table 5.9: MFC 8 calibration.

CH <sub>4</sub>				
Set point value [ml/min]	Measured value [ml/min]	Read value [ml/min]	Set point error [%]	Read error [%]
50	51.4	50.3	2.80	2.19
100	99.9	100	-0.100	0.299
200	199	200	-0.750	0.750

The results of calibration shown in the tables highlight the reduction of measurement errors (both reading and set point errors) as the quantity in [Nm<sup>3</sup>/min] of gas flowed inside the mass flow controllers increases. This condition is common to all measuring devices that have a much higher full scale value than the one measured in the testing phase.

The mass flow controller with a greater error both in terms of set up and reading error is the MFC 10 (the one used for CO gas, table 5.8). Instead, the mass flow

controller with lower error is the MFC 7 (table 5.6), dedicated to Nitrogen flow.

## 5.2 Setting up procedure

The preparation of the test bench is performed in accordance with the following procedure:

1. Wear appropriate protective equipment (PPE) provided in the lab: latex gloves, face mask.
2. Put all the components on a clear work surface checking the integrity. In this phase the components are cleaned and any obstruction is removed, for this purpose before the first use with a cell, the manifolds are fired to the intended test operation temperature for approximately two hours in order to burn out any residues from manufacturing and to create a protective oxide coating on the cathode manifold (figure 5.2).

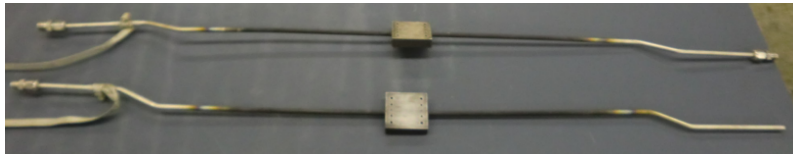


Figure 5.2: Cathode and Anode Manifolds representation.

3. Place the fresh manifolds in the furnace, for the first use cut and/or bend the inlet and outlet tubes if necessary to provide the best alignment.
4. Set up the tube so that the cathode inlet is on the same side as the anode exhaust, to create a cross flow configuration
5. In order to ensure good electrical contact apply a layer of silver ink to the manifold tube where the lead will make contact. Wrap the lead around the tube and apply a clamp to hold the lead to the tube. At the end each manifold has one current lead attached.
6. Place the anode manifold on a flat, stable surface and apply a small amount of superglue to all the four corners and insert a seal that covers them (figure 5.3).

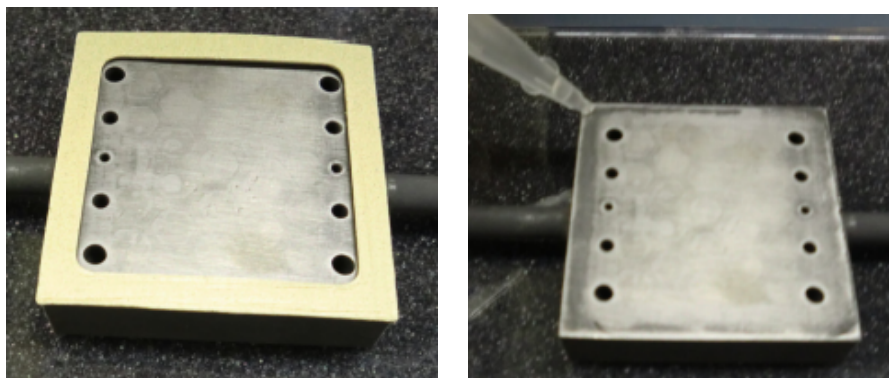


Figure 5.3: Superglue application and seal placing on the manifold.

7. Place the nickel mesh on the active area of the manifold making sure that does not overlap the seal or cover the gas flow ports (figure 5.4).

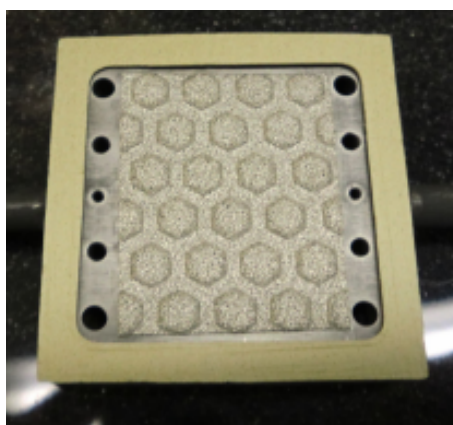


Figure 5.4: Mesh placing.

8. Cut the platinum voltage wire into two wires of sufficient length to extend the voltage monitoring connection. Bend a small hook into one platinum voltage wire and place it in the middle of the Ni mesh on the anode manifold.
9. Align, in a careful way the cell and place it anode side down in contact with voltage wire and nickel mesh (figure 5.5).

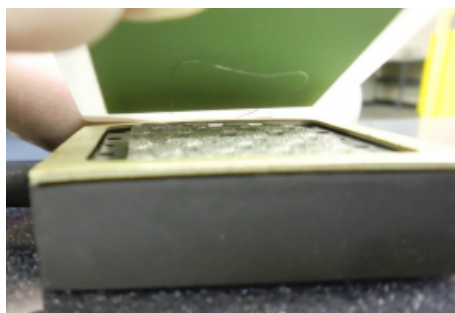


Figure 5.5: Cell alignment.

10. Place the remaining platinum voltage wire in the middle of the cathode active to measure the in-plane voltage.
11. Place the mesh in silver material onto cathode active area.
12. Place the remaining seal on the cell so that it is in alignment with the edge of the cell making sure the seal does not overlap the silver mesh (figure 5.6).

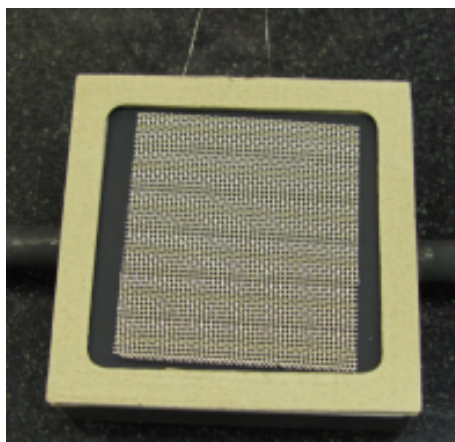


Figure 5.6: Mesh and seal placing onto cathode active area.

13. Place the anode manifold and cell inside the oven.
14. In order to separate the anode tubes from the cathode ones, place a small amount of flexible insulation between them (figure 5.7).



Figure 5.7: Collocation of the flexible insulation.

15. Place the cathode manifold on the anode manifold within and align it in the best way possible (figure 5.8).



Figure 5.8: Manifold alignment.

16. Add additional insulation if needed to isolate thermally the oven, as well as the anode and cathode tubes.
17. Place insulating ceramic cloth tubes over the anode and cathode voltage wires to isolate them from the oven (figure 5.9).



Figure 5.9: Insulating ceramic cloth tubes deployment.

18. Connect the voltage probes to the terminal board and current wires to the electronic load (the electrical connections are checked via voltmeter before closing the oven).
19. Close the oven with refractory bricks. To enhance the thermal insulation a ceramic plate is placed on the ceramic walls and it is covered with a layer of bricks.
20. The set-up is now complete.

The housing and the assembly of the test cell is reported in figure 5.10.

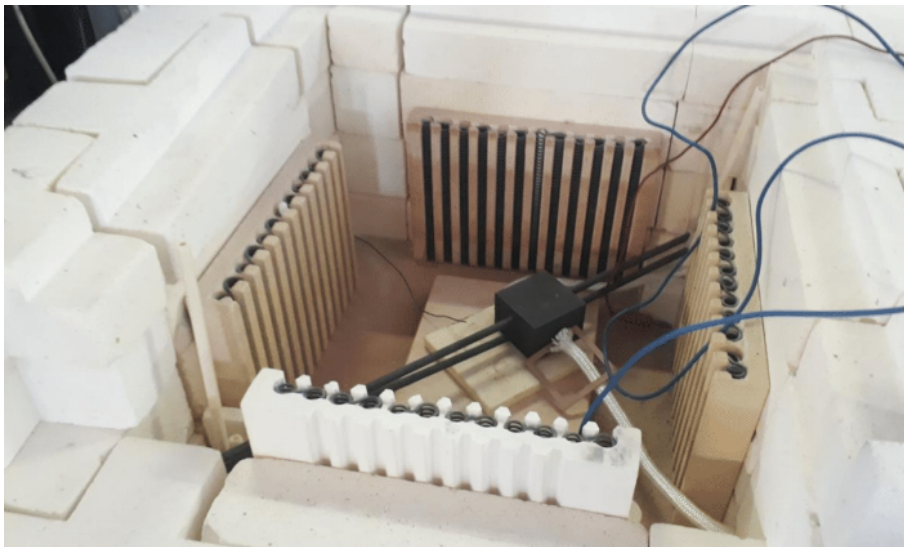


Figure 5.10: Housing of the test cell.

## 5.3 Start-up procedure

The start-up of the cell is based on three important phases; cell conditioning, cell reduction and activation. The following start-up procedures has been implemented during the experimental work.

### 5.3.1 Cell conditioning

The initial preparation of the cell involves the use of a protocol summarized below:

1. Switching on the fume hood.
2. Increase the anode flow to 150 [Nml/min] of dry  $N_2$  and the cathode flow to 150 [Nml/min] of air.
3. Program a temperature ramp that will heat up the oven to 850  $C^\circ$  in 14 hours ( 1  $C^\circ$ /min) and hold the temperature.
4. Start the Oven program.

This first phase of experimentation was carried out using a platform that is linked to the Teachy software explained in chapter 4.

This program (*Teachy script editor*) allows to write a script and convert it into a .json file. In this way the file can be loaded by the Teachy software and executed in the script section. The figure 5.11 shows the start-up script built in *Teachy script editor* platform. The first two commands displayed in the figure enable the setting of the required gas flows using mass flow controllers (in this case MFC5 and MFC7). In particular this two first rows are generated trough the window '*SETVARIABLE*' by writing the name of the desired variable to be set (which must be equal to the one present in Teachy software) and the value in [Nml/min] as shown in figure 5.12. Instead the last two rows in figure 5.11 allow to heat up the oven and keep the temperature high over time. In this case to create these commands the '*EurothermRLD*' window needs to be open (figure 5.13). Trough the first row the oven warm-up begins, with a ramp of 60  $C^\circ$ /h up to 300  $C^\circ$ . The second row enable the oven to reach 850  $C^\circ$  with a slower ramp of 30  $C^\circ$ /h. At this point the temperature level is stabilized for about 6 hours.

### 5.3.2 Cell reduction and activation

The last start-up phase of the cell is based on its reduction and activation. Cell reduction and activation occurs following a standard procedure:

1. Set up the  $N_2$  flow to 150 [Nml/min] and the  $H_2$  flow to 50 [Nml/min] on the anode side.

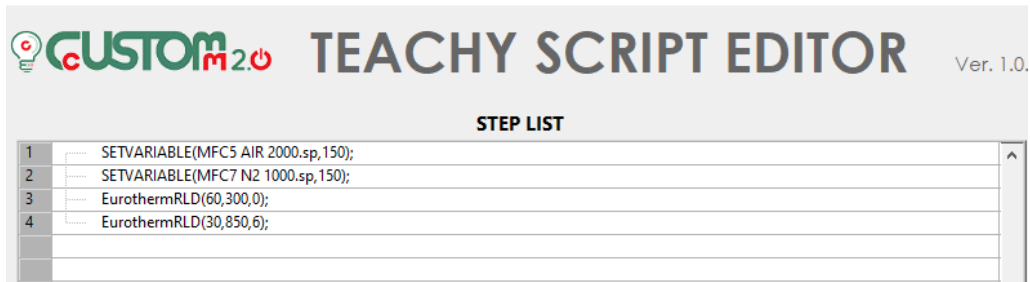


Figure 5.11: Start-up script.

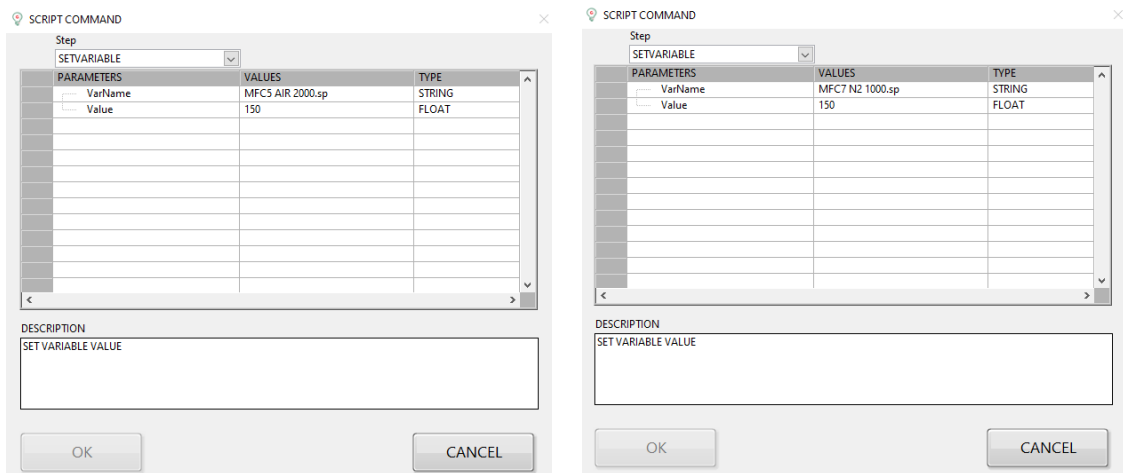


Figure 5.12: Setup variables windows.

2. Increase the cathode air flow to 250 [Nml/min].
3. Wait for a period of time of 30 minutes to ensure the stabilisation of the OCV (open circuit voltage).
4. Increase the  $H_2$  flow to 75 [Nml/min] and wait for another 10 minutes.
5. From 75 [Nml/min] increase the  $H_2$  flow to 225 [Nml/min] with increments of 50 [Nml/min] and at same time reduce the  $N_2$  flow from 150 to 0 [Nml/min], waiting in each step for the OCV stabilisation.
6. Increase the air flow up to 750 [Nml/min] in the cathode feed stream with even increments.
7. Once at the desired gas flows of 225 [Nml/min]  $H_2$ , 0 [Nml/min]  $N_2$  on the anode and 750 [Nml/min] of air on the cathode, wait for 15 - 30 minutes to assure steady state condition.

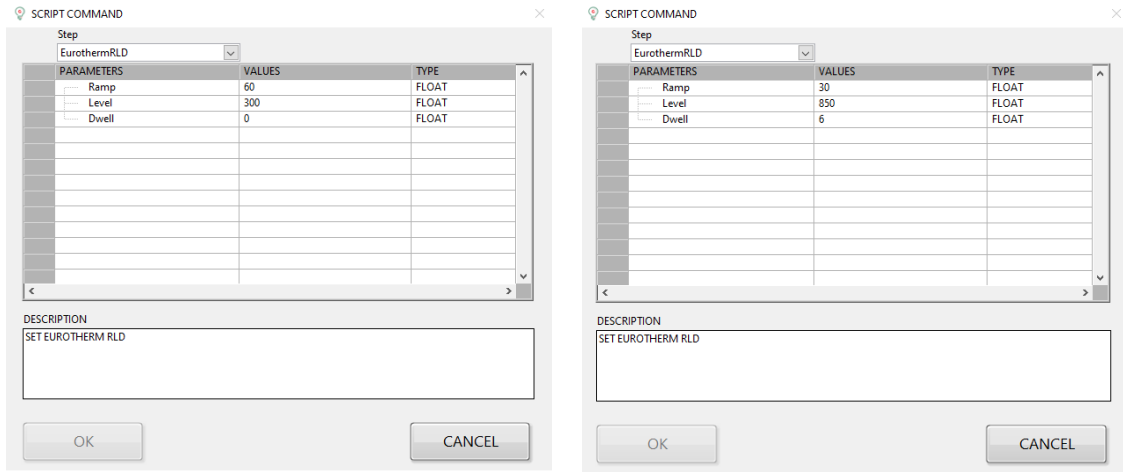


Figure 5.13: Eurotherm windows

- Setting a low value of current flow in the electrical circuit for a few hours to activate the cell.

The associated cell reduction script generated in *Teachy script editor* platform is illustrated in the figure 5.14.

For what concern the *'wait'* instruction, is created trough the window *'WAIT'* by writing the desired time in seconds.

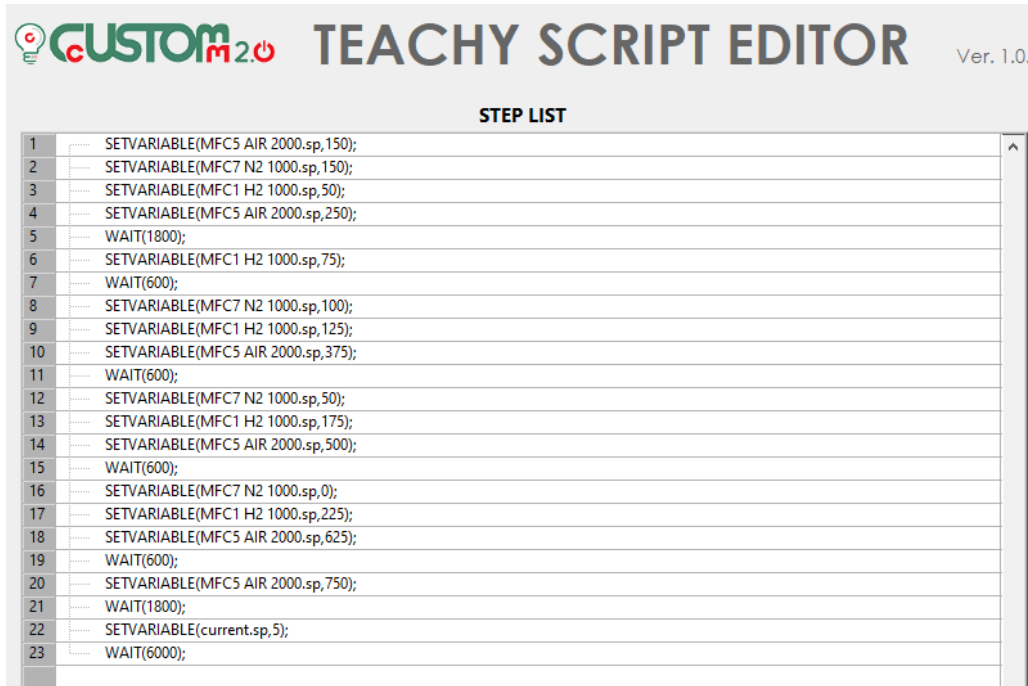
## 5.4 Cell testing

The tested planar cell has the following specifications:

- The Anode Electrode is made of NiO-GDC/NiO-YSZ materials, with geometries of 4 cm x 4 cm and 50  $\mu\text{m}$  of thickness.
- The Electrolyte Support is made of Hionic material (scandium stabilized zirconia) with geometries of 5 cm x 5 cm and 0.13-0.17 mm of thickness.
- The Cathode Electrode is made of LSM/LSM-GDC materials, with geometries of 4 cm x 4 cm and 50  $\mu\text{m}$  of thickness.

The cell testing session can be divided in two sections:

- Flow setting: working in SOEC mode, there is the necessity to increase the quantity of water at the expense of hydrogen. The CEM will increase the temperature with the water flow to ensure the vaporization.



The screenshot shows the 'CUSTOM m2u TEACHY SCRIPT EDITOR' interface, version 1.0. The main area is titled 'STEP LIST' and contains a table with 23 rows. Each row represents a step in the script, consisting of a step number and a command. The commands are a mix of 'SETVARIABLE' and 'WAIT' instructions with various parameters.

Step	Command
1	SETVARIABLE(MFC5 AIR 2000.sp,150);
2	SETVARIABLE(MFC7 N2 1000.sp,150);
3	SETVARIABLE(MFC1 H2 1000.sp,50);
4	SETVARIABLE(MFC5 AIR 2000.sp,250);
5	WAIT(1800);
6	SETVARIABLE(MFC1 H2 1000.sp,75);
7	WAIT(600);
8	SETVARIABLE(MFC7 N2 1000.sp,100);
9	SETVARIABLE(MFC1 H2 1000.sp,125);
10	SETVARIABLE(MFC5 AIR 2000.sp,375);
11	WAIT(600);
12	SETVARIABLE(MFC7 N2 1000.sp,50);
13	SETVARIABLE(MFC1 H2 1000.sp,175);
14	SETVARIABLE(MFC5 AIR 2000.sp,500);
15	WAIT(600);
16	SETVARIABLE(MFC7 N2 1000.sp,0);
17	SETVARIABLE(MFC1 H2 1000.sp,225);
18	SETVARIABLE(MFC5 AIR 2000.sp,625);
19	WAIT(600);
20	SETVARIABLE(MFC5 AIR 2000.sp,750);
21	WAIT(1800);
22	SETVARIABLE(current.sp,5);
23	WAIT(6000);

Figure 5.14: Cell reduction and activation script.

2. Polarization: the current flowing in the cell is gradually increased from 0 with steps of 1 A with a duration of 1 minute per step. The current increment is stopped when the average voltage rise above 1500 mV in order to avoid damaging the structure of the cell.

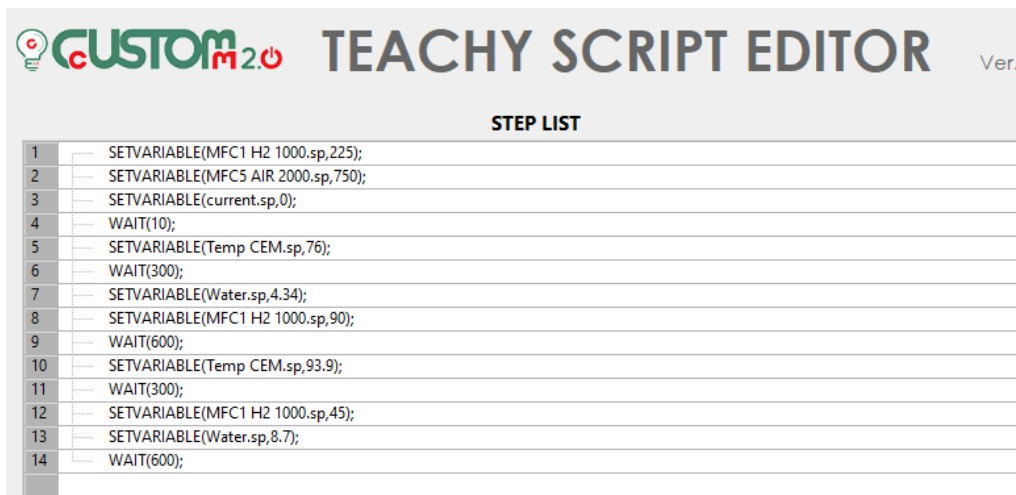
### 5.4.1 Flow setting

The procedure used to achieve a correct mixture in the anode area is based on increasing the quantity of water in g/h with steps of 20% at the expense of a reduction of the same amount of hydrogen from 225 [Nml/min] to 45 [Nml/min]. The calculation of the CEM temperature (shown in table 5.10) as a function of the quantity of water flow is crucial. The temperature computation is done through the CEM bronkhorst website.

The associated cell reduction script generated in *Teachy script editor* platform is illustrated in the figure 5.15.

Table 5.10: CEM flow mixture and temperature computation.

$H_2$ [Nml/min]	$H_2O$ [g/h]	Temperature [ $C^\circ$ ]
225	0	20.0
180	2.17	60.1
135	4.34	76.0
90.0	6.50	86.3
45.0	8.67	93.9



The screenshot shows the 'TEACHY SCRIPT EDITOR' interface. At the top, there is a logo for 'CUSTOM m2.0' and the text 'TEACHY SCRIPT EDITOR Ver.'. Below this is a 'STEP LIST' table with 14 rows, each containing a step number and a script command.

STEP	SCRIPT
1	SETVARIABLE(MFC1 H2 1000.sp,225);
2	SETVARIABLE(MFC5 AIR 2000.sp,750);
3	SETVARIABLE(current.sp,0);
4	WAIT(10);
5	SETVARIABLE(Temp CEM.sp,76);
6	WAIT(300);
7	SETVARIABLE(Water.sp,4.34);
8	SETVARIABLE(MFC1 H2 1000.sp,90);
9	WAIT(600);
10	SETVARIABLE(Temp CEM.sp,93.9);
11	WAIT(300);
12	SETVARIABLE(MFC1 H2 1000.sp,45);
13	SETVARIABLE(Water.sp,8.7);
14	WAIT(600);

Figure 5.15: SOEC flow setting.

## 5.4.2 Polarization

The experimental work continues with the polarization test. As mentioned in the previous chapters, the increase in the production of hydrogen in the electrolyser involves a greater work spent, this translates into a higher voltage value. To simulate this cell operating condition, the current is increased in steps of 1 A up to a maximum voltage limit (1500 mV). The evolution of the current versus voltage gives the polarization curve. This last phase of experimentation was abruptly stopped due to the breaking of the cell. The corresponding result analysis highlights how the SOEC

strongly degrades during the operation.

## 5.5 Shut-down procedure

The last point of the experimental work is related to the shut-down of the test bench. The following standard procedure is used:

1. Set up the  $N_2$  flow to 150 [Nml/min] in the anode side and the air flow to 150 [Nml/min] in the cathode side.
2. Program a temperature ramp that will cool down the oven to 20  $C^\circ$  with a ramp of 30  $C^\circ/h$
3. Run the script.

The associated shut-down script generated in *Teachy script editor* platform is illustrated in the figure 5.16.

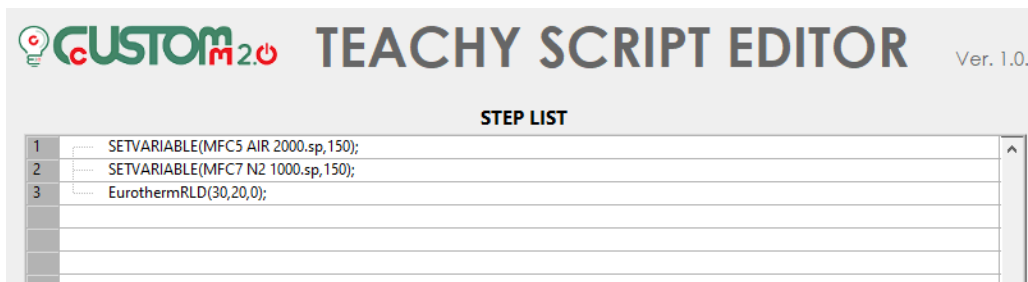


Figure 5.16: SOEC shut-down.

# Conclusions

The main objective of this work was based in testing an high temperature solid oxide cell. The behaviour of SOEC were studied both from theoretical and the experimental point of view.

The thermodynamic analysis has highlighted the principal features that characterize the cell, all the advantages and disadvantages of high temperature operation are investigated. Among all the benefits, the potential to decrease the electricity demand and to improve the kinetic reaction compared to low temperature electrolysis are the most remarkable. In contrast, the system's components must meet particular requirements to operate efficiently in this high challenging environment, this implies fairly higher cost and more complex fabrication. The cell performance was evaluated examining the polarization curve and the main operative losses. Possible modifications of the SOEC/SOFC structure have been outlined to reduce the irreversibility.

Experimental activity were performed on the test bench examining in details the main components and their role within the system. Special attention has been given to the acquisition and control system, in particular to the *Labview*-based control software, which is implemented in the *CompactRIO* (National Instrument) and connected to a remote server for data storage and web-interface management. To simulate the *Labview* software operation in the test bench, a simple system consisting of flow meters / controllers, thermocouples, a data acquisition system and input / output modules was implemented. The experimental activity has proved the feasibility of the system both to acquire physical measurements and to control the deployed instruments.

To remotely control the test rig, *Teachy* software has been used. The working principle is based on the communication between the local PLC (*compactRIO*) and virtual machine, where the control software is installed, achieved by Ethernet protocols. The experimental work was carried out analyzing the the various software sections through system command / response tests to provide improvements to the

*Teachy* software making the system easier to use by an operator.

The last part of the experimental work was based on the assembly and the analysis of the cell, both stages have been performed using standard procedures. This procedures have been converted into .json files by (*Teachy script editor*) platform to be executed in *Teachy* software. The analysis of the SOEC was carried out in two steps. The first step was based on achieving the desired mixture in the anode area (CEM temperature calculation). In the second step was simulated the cell operating condition, trying to generate a *Polarization curve* by increasing with steps of 1 A the current up to a maximum voltage limit. This last phase of experimentation was abruptly stopped due to the breaking of the cell, since it was already damaged with previous tests in SOFC mode.

The result of the analysis showed how the cell test was successful (at least in the SOFC case), but also how the high temperature electrolytic cells strongly degrades during the operation. In general, the solid oxide electrolysis can be considered an advanced technology with a high margin of development through further improvements on the existing materials and a reduction of component costs.

# Bibliography

- [1] Meng Ni et al. “Potential of renewable hydrogen production for energy supply in Hong Kong”. In: *International journal of hydrogen energy* 31.10 (2006), pp. 1401–1412.
- [2] Andrew L Dicks and David AJ Rand. *Fuel cell systems explained*. John Wiley & Sons, 2018.
- [3] Kavan Motazedi et al. “Economic and environmental competitiveness of high temperature electrolysis for hydrogen production”. In: *International Journal of Hydrogen Energy* 46.41 (2021), pp. 21274–21288.
- [4] Sonja van Renssen. “The hydrogen solution?” In: *Nature Climate Change* 10.9 (2020), pp. 799–801.
- [5] W Feduska and AO Isenberg. “High-temperature solid oxide fuel cell—technical status”. In: *Journal of power sources* 10.1 (1983), pp. 89–102.
- [6] “SOFC working principle”. URL: [https://en.wikipedia.org/wiki/Solid\\_oxide\\_fuel\\_cell](https://en.wikipedia.org/wiki/Solid_oxide_fuel_cell).
- [7] SH Chan, KA Khor, and ZT Xia. “A complete polarization model of a solid oxide fuel cell and its sensitivity to the change of cell component thickness”. In: *Journal of power sources* 93.1-2 (2001), pp. 130–140.
- [8] Anthony L Hines and Robert N Maddox. *Mass transfer: fundamentals and applications*. Vol. 434. Prentice-Hall Englewood Cliffs, NJ, 1985.
- [9] V Utgikar and Todd Thiesen. “Life cycle assessment of high temperature electrolysis for hydrogen production via nuclear energy”. In: *International Journal of Hydrogen Energy* 31.7 (2006), pp. 939–944.
- [10] Andreas Patyk, Till M Bachmann, and Annabelle Brisse. “Life cycle assessment of H<sub>2</sub> generation with high temperature electrolysis”. In: *International Journal of Hydrogen Energy* 38.10 (2013), pp. 3865–3880.
- [11] MS Sohal et al. *Challenges in generating hydrogen by high temperature electrolysis using solid oxide cells*. Tech. rep. Idaho National Laboratory (INL), 2008.

- [12] Meng Ni, Michael KH Leung, and Dennis YC Leung. “Technological development of hydrogen production by solid oxide electrolyzer cell (SOEC)”. In: *International journal of hydrogen energy* 33.9 (2008), pp. 2337–2354.
- [13] Junyoung Kim et al. “Hybrid-solid oxide electrolysis cell: A new strategy for efficient hydrogen production”. In: *Nano Energy* 44 (2018), pp. 121–126.
- [14] Sossina M Haile. “Fuel cell materials and components”. In: *Acta materialia* 51.19 (2003), pp. 5981–6000.
- [15] Shunrun Chen et al. “Controlling the redox reaction at the interface between sealing glasses and Cr-containing interconnect: Effect of competitive reaction”. In: *Journal of Power Sources* 267 (2014), pp. 753–759.
- [16] Jochen Schilm et al. “Ceramic integration technologies for solid oxide fuel cells”. In: *International Journal of Applied Ceramic Technology* 9.4 (2012), pp. 688–699.
- [17] “Glass sealing material”. URL: <https://mo-sci.com/novel-sealants-improve-solid-oxide-fuel-cells/>.
- [18] “MFC working principle”. URL: [https://www.bronkhorst.com/getmedia/98668a82-8d1c-4b7f-af8e-995be25641b3/EL-FLOW-Select\\_en.pdf](https://www.bronkhorst.com/getmedia/98668a82-8d1c-4b7f-af8e-995be25641b3/EL-FLOW-Select_en.pdf).
- [19] “CEM working principle”. URL: <https://www.bronkhorst.com/int/service-support-1/technologies/theory-and-advantages-of-cem-vapour-control/>.
- [20] “eurotherm”. URL: <https://www.eurotherm.com/it/products/temperature-controllers-it/single-loop-temperature-controllers-it/2400-temperature-controller-programmer/>.
- [21] “PID control”. URL: <https://www.eurotherm.com/it/temperature-control-it/principles-of-pid-control-and-tuning/>.
- [22] “LabVIEW”. URL: <https://en.wikipedia.org/wiki/LabVIEW>.
- [23] “LabVIEW”. URL: [https://neurophysics.ucsd.edu/Manuals/National%20Instruments/LV\\_Fundamentals.pdf](https://neurophysics.ucsd.edu/Manuals/National%20Instruments/LV_Fundamentals.pdf).
- [24] “Definer”. URL: <https://worldindustrialreporter.com/gas-flow-meter-definer-220/>.

# Acknowledgments

Alla fine di questo percorso fatto di gioie, dolori, ansie e traguardi, le prime persone che mi vengono in mente sono i miei genitori.

Ricordo appena quel giorno di fine settembre di 2 anni fa quando dovetti partire per Torino, immagino quando sia stato difficile per loro salutarmi, malgrado siano stati i primi a incoraggiarmi. Non posso fare altro che ringraziarli per tutti i loro sacrifici, ma soprattutto per aver creduto in me.

Un ringraziamento speciale va ai miei fratelli e ai miei zii, ma in modo particolare a mio fratello gemello Simone. Anche se la vita ci ha allontanato è il primo con cui condivido gioie e dolori, sono molto orgoglioso di lui e della strada che sta percorrendo.

Un grazie va alla mia ragazza Giorgia, per esserci stata sempre, nei momenti più belli e soprattutto in quelli più difficili del mio percorso.

Ringrazio il mio correlatore Domenico Ferrero e il mio relatore Massimo Santarelli, per avermi fatto conoscere più da vicino il mondo dell'idrogeno e le sue applicazioni.

Infine un grazie va a tutti i miei amici, Roberto, Antonio, Davide, Alessadro, Vittorio, Francesco, Fernando e al mio collega nonché compagno di progetti Emanuele.

Dedico il mio percorso universitario ai miei nonni, che mi guardano da lassù, ci siamo lasciati quando ero solo un bambino, spero siate orgogliosi dell'uomo che sono diventato.